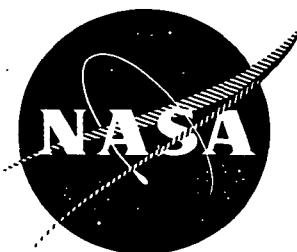


N 73 27799

NASA CR-121239

036390-2-T

**CASE FILE
COPY**



PRELIMINARY MEASUREMENTS ON HEAT BALANCE IN PNEUMATIC TIRES

**G. H. NYBAKKEN
D. Y. COLLART
R. J. STAPLES**

**J. I. LACKEY
S. K. CLARK
R. N. DODGE**

**COLLEGE OF ENGINEERING
DEPARTMENT OF APPLIED MECHANICS AND ENGINEERING SCIENCE
DEPARTMENT OF MECHANICAL ENGINEERING
TIRE AND SUSPENSION SYSTEMS RESEARCH GROUP
THE UNIVERSITY OF MICHIGAN
ANN ARBOR, MICHIGAN 48105**

July 1973

**Prepared for
AEROSPACE SAFETY RESEARCH AND DATA INSTITUTE
LEWIS RESEARCH CENTER
NATIONAL AERONAUTICS AND SPACE ADMINISTRATION**

**Under
NASA Grant NGR 23-005-417**

1. Report No. NASA CR-121239.		2. Government Accession No.		3. Recipient's Catalog No.	
4. Title and Subtitle Preliminary Measurements on Heat Balance in Pneumatic Tires				5. Report Date July 1973	
				6. Performing Organization Code	
7. Author(s) G. H. Nybakken, D. Y. Collart, R. J. Staples, J. I. Lackey, S. K. Clark, R. N. Dodge				8. Performing Organization Report No. 036390-2-T	
9. Performing Organization Name and Address The University of Michigan College of Engineering Ann Arbor, Michigan 48105				10. Work Unit No.	
				11. Contract or Grant No. NRG 23-005-417	
12. Sponsoring Agency Name and Address National Aeronautics and Space Administration Washington, D.C. 20546				13. Type of Report and Period Covered Contractor's Report	
				14. Sponsoring Agency Code	
15. Supplementary Notes Technical Monitor: C. D. Miller Aerospace Safety Research and Data Institute NASA Lewis Research Center, Cleveland, Ohio 44135					
16. Abstract A variety of tests was undertaken to determine the nature of heat generation associated with a pneumatic tire operating under various conditions. Tests were conducted to determine the magnitude and distribution of internally generated heat caused by hysteresis in the rubber and ply fabric in an automobile tire operating under conditions of load, pressure, and velocity representative of normal operating conditions. These included tests at various yaw angles and tests with braking applied. In other tests, temperature sensors were mounted on a road to measure the effect of a tire rolling over and an attempt was made to deduce the magnitude and nature of interfacial friction from the resulting information. In addition, tests were performed using the scratch plate technique to determine the nature of the motion between the tire and road. Finally, a model tire was tested on a roadwheel, the surface covering which could be changed, and an optical pyrometer was used to measure rubber surface temperatures.					
17. Key Words (Suggested by Author(s)) Hysteresis Heating Model Tire Studies Pneumatic Tire Tire Friction			18. Distribution Statement Unclassified, Unlimited		
19. Security Classif. (of this report) Unclassified		20. Security Classif. (of this page) Unclassified		21. No. of Pages 74 + vi	
				22. Price* \$3.00	

* For sale by the National Technical Information Service, Springfield, Virginia 22151

Page Intentionally Left Blank

FOREWORD

This report has been prepared by the Tire and Suspension Systems Research Group, Department of Applied Mechanics and Engineering Science and Department of Mechanical Engineering, College of Engineering, The University of Michigan, Ann Arbor, Michigan under Grant No. NGR 23-005-417 from the Lewis Research Center, National Aeronautics and Space Administration, Cleveland, Ohio 44135. Mr. C. David Miller of the Lewis Research Center served as technical monitor. The work was performed under the direction of Professor S. K. Clark of The University of Michigan

The use of SI units (NASA Policy Directive NPD 2220.4, September 14, 1970) was waived for the present document in accordance with the provisions of paragraph 5d of that directive by the authority of the Director of the Lewis Research Institute.

TABLE OF CONTENTS

	Page
LIST OF ILLUSTRATIONS	v
I. SUMMARY	1
II. INTRODUCTION	2
III. THERMOCOUPLE MEASUREMENTS	3
IV. TEMPERATURE SENSOR MEASUREMENTS	21
V. SCRATCH PLATE MEASUREMENTS	37
VI. MODEL TIRE STUDIES	39
VII. SUMMARY OF RESULTS	61
VIII. APPENDIX 1. THEORETICAL ANALYSIS OF SENSOR	65
IX. APPENDIX 2. ALTERNATE METHOD OF CALCULATING HEAT GENERATION	72
X. REFERENCES	74

LIST OF ILLUSTRATIONS

Table	Page
I. Summary of Experiments with Free Rolling Tires	11
II. Summary of Experiments with Yawed and Braked Tires	12
III. Summary of Experiments with H78-15 Tire at 30 mph	13
IV. Summary of Experiments	14

Figure

1. Thermocouple locations relative to cross section for G78-15 #5 and #8 6JK rim.	15
2. Thermocouple relative to cross section for H78-15 on 6JK rim (shown on a tracing of a G78-15 on a 6JK rim).	16
3. Temperature build-up around cross section.	17
4. Temperature build-up within crown.	18
5. Temperature profiles at crown.	19
6. Heat generation profile at crown.	20
7. Detail of sensor construction.	31
8. Sensor mounted on pavement.	31
9. Sensor array on pavement.	32
10. Treadless test tire mounted on truck.	32
11. Tire path record for Trial 6.	33
12. Tire path record for Trial 8.	34
13. The response of the sensor to a heat flux pulse.	35
14. Heat flux pulse of constant unit magnitude.	36
15. (a) and (b) Positional information for surface temperature measurements; (c) tire as viewed from top.	44

LIST OF ILLUSTRATIONS (Continued)

Figure		Page
16.	Surface temperatures at various positions vs. speed on cast iron at 0° yaw.	45
17.	Surface temperatures at various positions vs. speed on sanded Safety Walk at 0° yaw.	46
18.	Surface temperatures at various positions vs. speed on cast iron and sanded Safety Walk at 0° yaw.	47
19.	Temperature change of tension shoulder after going through contact patch vs. speed.	48
20.	Temperature change of center tread after going through contact patch vs. speed.	49
21.	Temperature difference between compressed shoulder and tensioned shoulder vs. speed.	50
22.	Temperature difference between compressed sidewall and tensioned sidewall vs. speed.	51
23.	Center tread temperature entering contact patch.	52
24.	Center tread temperature leaving contact patch.	53
25.	Compression sidewall temperature entering contact patch.	54
26.	Tension sidewall temperature entering contact patch.	55
27.	Compression shoulder temperature entering contact patch.	56
28.	Tension shoulder temperature entering contact patch.	57
29.	Temperature difference of center tread (and tension shoulder) between cast iron and sanded Safety Walk.	58
30.	Drag load in wheel plane vs. speed.	59
31.	Drag load in direction of motion vs. speed.	60
32.	Detail of sensor installation.	70
33.	Schematic of sensor installation.	70
34.	Analog of sensor installation for theoretical analysis.	70
35.	Temperature/flux in nickel as a function of time.	71

I. SUMMARY

The purpose of the tests reported here was to examine the nature and magnitude of the heat generated by a pneumatic tire and to determine how the energy dissipated was partitioned into the two major avenues of heat generation: heat generation caused by inter-ply friction and hysteresis in the rubber carcass and heat generation at the rubber-road interface caused by friction and motion between the contacting surfaces.

In one series of tests a full size automobile tire was instrumented by imbedding thermocouples in the carcass and the time rate of change of temperature was measured under conditions similar to the normal operating conditions for the tire. Simple calculations then yielded a measure of the magnitude and location of internally generated heat. The total energy losses were estimated or measured and some tentative estimates of the partitioning of the total dissipated energy were made.

In another series of tests attention was given to the nature and magnitude of the heat generated at the rubber-road interface. A technique utilizing temperature sensors bonded to the road surface was explored. This provided a measure of the flux of energy into the road when a full size, fully loaded automobile tire passed over. The results of these particular tests are difficult to interpret and some pertinent data is presented but no conclusions are drawn. A theoretical analysis of the response of the sensor to a step input is presented.

The scratch plate technique was used to study the interfacial motions between the rubber and the road and some estimates of interfacial heat generation were made.

In another series of experiments, a tire model was operated on a small roadwheel which had a cast iron surface. An optical pyrometer was used to measure steady state surface temperature at various locations around the circumference of the tire in the sidewall, shoulder, and crown regions. A similar series of tests was conducted with a sandpaper-like surface covering applied to the roadwheel. Both series were conducted over a range of speeds and drag force was measured.

II. INTRODUCTION

The purpose of the analysis and measurements outlined in this report is to give a clearer picture of the origin of heat generation in a pneumatic tire, and of the way in which the heat leaves the tire. In more detailed form, this question breaks down into several individual questions or research studies, each worthy of substantial effort.

These may be expressed as:

- (1) To what extent is heat generated by hysteresis within the tire tread and side walls, and to what extent by mechanical scuffing between outer tread surface and roadway?
- (2) What is the distribution of release of heat by hysteresis relative to depth beneath the outer tread surface?
- (3) To what extent does the total heat generated flow to the atmosphere, and to what extent does it flow through the contact patch into the roadway?

Subsequent sections of this report attempt to throw light on these questions by both analytical and experimental means.

III. THERMOCOUPLE MEASUREMENTS

A series of experiments was conducted to examine the internal heating of a tire carcass under various conditions. The tires were instrumented with thermocouples bonded into the carcass. The temperature was recorded as a function of time and from this data the rate of heat generation could be calculated. This rate of heat generation can be compared to the mechanical power dissipated.

The experiments were conducted on regular roads using The University of Michigan Highway Safety Research Institute Mobile Tire Tester, a truck modified to carry a tire under various loads and alignments at normal highway speeds.

A total of three tires was instrumented and yielded useful information in the tests. Two of the tires, identical B. F. Goodrich G78-15 bias belted tubeless tires mounted on 6JK pressed steel rims, were instrumented in the same way. They bore code numbers DG24-0026-5 G598 and DG24-0026-8 G598 and are identified by the abbreviations G78-15 #5 and G78-15 #8, respectively. These two tires had a solid tread surface with the same gross contour as the standard production tire, but without grooves or sipes. The third tire was an H78-15 of the same construction as the G78-15 tires and was mounted on the same rim. This tire had a standard production tread. All three tires were load range B tires and the two sizes are both common on domestic intermediate size automobiles.

The thermocouple locations relative to a cross-section for the G78-15 tires and the H78-15 tire are shown in Figures 1 and 2, respectively.

The tires carried 1000-lb vertical load and were inflated to 24 psi except as otherwise noted.

The thermocouples were installed in the following way: the immediate area of the chosen location was frozen with liquid nitrogen, a 1/8 in. hole was drilled to the proper depth, the tire was allowed to return to room temperature, the thermocouple was inserted, and the hole was potted with Duro Plastic Rubber (T.M.). The Plastic Rubber was injected with a syringe to avoid trapping air pockets.

All holes were drilled from the inside of the tire. In those locations where the thermocouple was within or beyond the ply structure it was necessary to drill through the fabric.

Those thermocouples located on the interior wall of the carcass were glued with Plastic Rubber into shallow dimples machined into the surface.

The thermocouples were made from 28-gauge copper-constantan twin lead wire with plastic insulation. The junctions were butt-welded electrically and that region stripped of insulation during the welding process was coated with "Gaugecoat," a thin latex rubber waterproofing agent.

The wire leads extended from the point where they emerged from the rubber, around the inside of the tire to the common exit holes in the rim. There were two such exit holes for the G78-15 tires and one for the more lightly instrumented H78-15 tire. The wires passed through the holes in a bundle and the hole region was potted with Plastic Rubber which served as a grommet, seal, and mechanical reinforcement.

The lead wires were fastened to the inside of the tire at 6-in. intervals using tape secured with Eastman 910 adhesive. Preliminary experiments showed that a small amount of slack between these fastening points was necessary to permit the lead wires to flex with the tire and to prevent breakage.

The constantan lead wires were fastened to a common junction inside the tire cavity and a single constantan lead wire was brought out from this junction.

After passing through the exit holes the wire bundle was brought to a slip ring assembly, thence to a 32°F ice bath reference junction located on the rear of the truck, and finally to the instrumentation in the cab of the truck.

The instrumentation in the truck consisted of a low resistance multipole switch, a digital microvolt meter, a stop watch, and a tape recorder. The switch position and corresponding voltage and time were read verbally into the recorder for later transcription.

The experiments reported here were performed on three occasions. The experiments using the H78-15 tire were performed on November 19, 1970, and December 3, 1970, at Ann Arbor, Michigan, on concrete roads with air temperatures between 40° and 45°F. The experiments using the G78-15 tires were performed March 1, 1971, through March 3, 1971, inclusive, at College Station, Texas, on asphalt roads with air and road temperatures in the ranges 40° - 70°F and 45° - 90°F, respectively.

The experiments were conducted by bringing the truck to the appropriate speed, at which point the tire was lowered to the pavement and run under load at a constant speed until the appropriate data

had been taken. The tire was then lifted and allowed to reach a uniform temperature as determined by the thermocouples before a second experiment was conducted.

The recorded thermocouple potentials were transcribed and converted to degrees Fahrenheit and plotted as temperature vs. time. The data for the initial 1 to 2 min were examined to determine if conduction, diffusion, and convection effects were sufficiently small to warrant further processing of the data. If the graphs were sufficiently straight and did not exhibit curvature or the exponential leveling off associated with heat flow, then it was assumed that the rate of temperature increase was representative of the initial input of heat.

It should be noted that, barring heat flow, the conversion of a constant mechanical power input to thermal energy yields a constant rate of temperature increase independent of initial temperature of the tire, and the ambient road and air temperatures.

The rate of temperature increase was determined by fitting a straight line to the temperature vs. time graph and determining the slope of this line or by taking the temperature difference between two data points spaced 60 or 80 sec apart and directly calculating $\Delta T/\Delta t$. The two methods are almost equivalent and the choice of method was subjectively according to the appearance of the graphs. The time interval in either case was centered about the 40-60 sec region.

The rate of temperature increase can be converted to a rate of thermal energy release using a simple formula:

$$Q = \Delta T / \Delta t \cdot C \cdot M$$

where

Q = Thermal energy influx Btu/sec

C = Specific heat capacity Btu/ $^{\circ}$ F lbm

M = Mass, lbm

Two schemes were used to perform this conversion. In the first scheme the simple average $\Delta T / \Delta t$ from thermocouples located throughout the tire was used and the mass was that of the entire tire. The tire weighed 30 lb and, using a specific heat capacity of .48 Btu/ $^{\circ}$ F \cdot lbm, the formula becomes

$$Q = 11200 \Delta T / \Delta t \quad (1)$$

where Q is in ft-lb/sec and $\Delta T / \Delta t$ in $^{\circ}$ F/sec.

In the second scheme the tire cross section was partitioned geometrically into sections centered around the thermocouples and the sum of the heat generated within each of these sections yielded a weighted average heat influx over the tire.

The first scheme, although much less precise than the second, yielded almost the same value and because the first scheme was much easier to use and because the difference between the values obtained using the two schemes was less than the overall projected uncertainty

in the whole experiment, it was decided to use the first scheme for all the calculations of heat influx.

The second scheme is illustrated in Appendix 2. The partitioned sections used are shown in Figure 1.

Experiments were conducted with the tires unyawed and rolling free, with the tires at yaw angles of 4° and 8° , and with brake torques yielding drag forces up to 460 lb. The speeds used were 30 and 50 mph. Drag force could be measured for either nonzero yaw or nonzero brake torque but was too small to be measured for the free rolling case. The drag of the unyawed free rolling tire was assumed to be 20 lb, equal to 2% of the 1000-lb vertical load because it was not possible to measure the drag.

Samples of the data and the graphs derived from them are shown in the figures and tables.

Figure 3 gives an example of the temperature vs. time data for thermocouples located around the cross section and Figure 4 gives an example of temperature vs. time data for points within the crown and on the inside wall. Both these figures refer to a free rolling tire.

Figures 5 and 6 show sample temperature and heat generation profiles, respectively, through the crown of the tire. The specific rate of heat generation is the product of the rate of temperature increase and the specific heat capacity, neglecting heat flow.

The total heat generation data for the free rolling tire is presented in Table I along with the power input based on 20 lb drag and 50 mph forward speed. The heat generation is calculated according to Eq. (1). The relatively good agreement between the thermally

calculated drag and the assumed mechanical drag may be accidental since the mechanical drag of a cold tire is not readily available. The mean deviation for the $\Delta T/\Delta t$ data is 9% and it follows that the same mean deviation is applicable to the Q values. If the drag was indeed constant for all the experiments the average Q/P value has a mean deviation of 9%. This fact coupled with the average Q/P value of 1.035 indicates that the majority of mechanical energy used to drive a free rolling tire is converted to heat via tire rubber and fabric hysteresis.

The data in Table II represent the heat generation around the cross section for various yaw and braking conditions for the G78-15 #5 tire. The drag was measured using the equipment on the Mobile Tire Tester. The power expenditure is meaningful only for the yawed experiments because in the braked experiments the brake mechanism absorbs an unknown fraction of the total mechanical energy.

However, the yawed experiments may be compared with the unyawed experiments. Here we see that only 36% of the assumed mechanical energy is converted into carcass heat whereas the figure for an unyawed tire was close to 100%. The difference is apparently due to the increased scrubbing in the contact patch in the yawed case.

Table III contains a summary of some pertinent experiments with the H78-15 tire which was instrumented in the shoulder region. The experiments were all conducted at 30 mph with the standard 1000-lb vertical load and 24 psi inflation pressure. The heat generation rate Q was determined by using Eq. (1). The thermocouple locations are

referenced in Figure 2. The power figure for the free rolling tire corresponds to 20 lb drag.

Note that the drag force may be under-estimated because the Q/P ratio indicates a surplus of 13%. However, the Q/P data for both the free rolling and yawed rolling tests compare well with the data for the corresponding tests with the G78-15 tires considering the extent of the uncertainties involved in the tests.

Most of the experiments were of less than 5 min total duration because diffusion and convection effects would only complicate the determination of heating effects as explained previously. However, one experiment was conducted for a time sufficient to reach thermal equilibrium. A summary of the experiments pertinent to this report is presented in Table IV.

Temperature profiles through the crown showing the approach to equilibrium are shown in Figure 5. Note that as conduction within the tire and heat transfer out of the tire become important, the hottest point in the crown moves from the region close to the surface inward toward the middle of the cross section. The profile yields temperature gradient data which indicates that at equilibrium about 78% of the radial heat flow is toward the outer surface and the remaining 22% is toward the inner surface.

TABLE I

SUMMARY OF EXPERIMENTS WITH FREE ROLLING TIRES

VALUES OF $\Delta T/\Delta t$, $^{\circ}\text{F}/\text{SEC}$ VS THERMOCOUPLE LOCATION

0° yaw, no braking; 50 mph

Test #8 with G78-15 #8; all other tests with G78-15 #5

Test	Thermocouple Number, Ref: Fig 1									Q, ft lb/sec	P, ft lb/sec	Q/P
	1	2	3	4	5	6	7	8	9			
6	.0875	.1875	.2000	.1250	.1188	.1250	.2063	.1250	.1570	.1570	1760	1.200
7	.625	.1438	.1313	.1188	.0688	.0938	.1688	.2250	.1000	.1263	1416	.965
11A	.1175	*	.2050	.1250	.0900	.1250	.2050	*	.1900	.1511	1692	1.152
13	.0775	*	.1613	.1188	.1025	.1238	.1950	*	.1088	.1268	1420	.968
1	.0688	.1375	.1250	.1000	.1063	.1125	.1688	.2063	.1125	.1264	1417	.965
8	.0625	.1750	.1063	.1188	.1313	.1375	.1500	.1438	.1375	.1290	1446	.986
Avg.	Average of six experiments →									.1357	1520	1.035

Q is calculated according to Eq. (1). It is the rate of increase of the total heat energy within the tire structure.

P is the product of the total drag and velocity.

*Thermocouple inoperative. This location omitted from average.

TABLE II

SUMMARY OF EXPERIMENTS WITH YAWED AND BRAKED TIRES
VALUES OF $\Delta T/\Delta t$, $^{\circ}\text{F}/\text{SEC}$ VS THERMOCOUPLE LOCATION

Tire G78-15 #5, 50 mph

Test	Yaw, deg	Brake*	Drag lb	Thermocouple Number, Ref: Fig 1								Q, ft lb/sec	P, ft lb/sec	Q/P
				1	3	4	5	6	7	9	Avg. of 1-9			
10	4	0	70	.1750	.2875	.1613	.1175	.1600	.1650	.0900	.1652	1850	5140	.360
12A	8	0	112	.2375	.3613	.2575	.2238	.2963	.2838	.1988	.2656	2970	8210	.362
11B	0	✓	70	.0775	.1475	.1050	.0863	.1050	.1913	.1000	.1161	1290	5140**	.252**
12B	0	✓	112	.0775	.1100	.0650	.0500	.0663	.1125	.0688	.0786	870	8210**	.106**

Q is calculated according to Eq. (1). It is the rate of increase of the total heat energy within the tire structure.

P is the product of the total drag and velocity.

*A check (✓) indicates that the brake was applied.

**No attempt has been made to determine the power dissipated in the braking system. Hence, this P does not represent power absorbed by the tire.

TABLE III

SUMMARY OF EXPERIMENTS WITH H78-15 TIRE AT 30 MPH
VALUES OF $\Delta T/\Delta t$, °F/SEC VS THERMOCOUPLE LOCATION

Test	Yaw, deg	Brake*	Drag lb	Thermocouple Number, Ref: Fig 2									Q, ft lb/sec	P, ft lb/sec	Q/P	
				1	2	3	4	5	6	7	8	9				Avg. of 1-9
18	0	0	D ₀ ^b	.0875	.1125	**	.1250	.0750	.0625	.0792	.0792	.0708	.0865	969	880	1.111
22 ^a	0	0	D ₀ ^b	.1083	.1125	.1250	.1167	.0833	.0708	.0750	.0667	.0625	.0912	1042	880	1.182
15	0	✓	100	.0778	.1278	**	.1444	.0944	.0778	.0889	.0889	.0778	.0972	1090	4400	.248
24 ^a	0	✓	100	.0611	.0833	**	.0944	.0611	.0389	.0500	.0500	.0444	.0604	628	4400	.154
17	4	0	90	.0944	.1000	**	.1667	.0722	.1556	.1722	.1444	.1444	.1312	1470	3960	.371
16	4	0	165	.1056	.1000	**	.2111	.0944	.2333	.2278	.2056	.2056	.1729	1935	7250	.267
23 ^a	8	0	90	.0889	.0833	**	.1556	.0667	.1667	.1566	.1167	.1222	.1195	1340	3960	.338
Avg. of 18, 22	0	0											.0889	995	880	1.130

Q is calculated according to Eq. (1). It is the rate of increase of the total heat energy within the tire structure.

P is the product of the total drag and velocity.

*A check (✓) indicates that the brake was applied.

**Thermocouple inoperative. This location omitted from average.

^aThese tests were conducted with an improperly sealed system. Pressure dropped from 29 psi to approximately 24 psi for these tests.

^bD₀ is taken to be 20 lb equal to 2% of 1000-lb vertical load.

TABLE IV

SUMMARY OF EXPERIMENTS

Data Page No.	Date	Tire*	Yaw, deg	Brake**	Drag, + lb	Side Force, ++ lb	Velocity, mph	T _{road} , °F	T _{air} , °F	Load, lb	Pressure, psi
1	3/ 1/71	8	0	-	D ₀	0	50	90	70	1000	22
2	3/ 1/71	8	4	-	64	647.5	50	95	70	1000	22
3	3/ 1/71	8	8	-	?	?	50	95	70	1000	24
4	3/ 2/71	14	0	-	D ₀	0	50	51	43	1000	24
5	3/ 2/71	14	0	-	D ₀	0	50	51	43	1000	24
6	3/ 2/71	5	0	-	D ₀	0	50	46	40	1000	24
7	3/ 2/71	5	0	-	D ₀	0	50	46	40	1000	24
8	3/ 2/71	5	0	-	D ₀	0	50	46	40	1000	24
9	3/ 3/71	5	0	-	D ₀	0	50	54	34	1000	24
10	3/ 3/71	5	4	-	70	?	50	65	41	1000	24
11A	3/ 3/71	5	0	-	D ₀	0	50	65	41	1000	24
11B	3/ 3/71	5	0	✓	70	0	50	70	46	1000	24
12A	3/ 3/71	5	8	-	112	?	50	70	46	1000	24
12B	3/ 3/71	5	0	✓	112	0	50	70	46	1000	24
13	3/ 3/71	5	0	-	D ₀	0	50	54	34	1000	24
14	3/ 3/71	5	0	-	D ₀	0	50	54	34	1000	24
15	12/ 3/70	H	0	✓	100	0	30	54	34	1000	24
16	12/ 3/70	H	8	-	165	814	30	54	34	1000	24
17	12/ 3/70	H	4	-	90	555	30	54	34	1000	24
18	12/ 3/70	H	0	-	D ₀	0	30	54	47	1000	24
19	This data page blank										
20	12/ 3/70	H	0	✓	460	0	40,50	54	47	1000	24
21	12/ 3/70	H	10	-	377	560	50	54	47	1000	24
22	11/19/70	H	0	-	D ₀	0	30	54	40	1000	28-18
23	11/19/70	H	4	-	90	555	30	54	40	1000	29-22
24	11/19/70	H	0	✓	100	0	30	54	40	1000	29-?
25	11/19/70	H	8	-	165	814	30	54	40	1000	24

*G78-15 #5 + 5

G78-15 #8 + 8

H78-15 + H

7.75-14 + 14

**A check (✓) indicates that the brake was applied.

*D₀ = Drag under free rolling conditions. This is assumed to be 20 lb and could not be measured accurately.

++Side force is assumed to be zero in all unyawed cases.

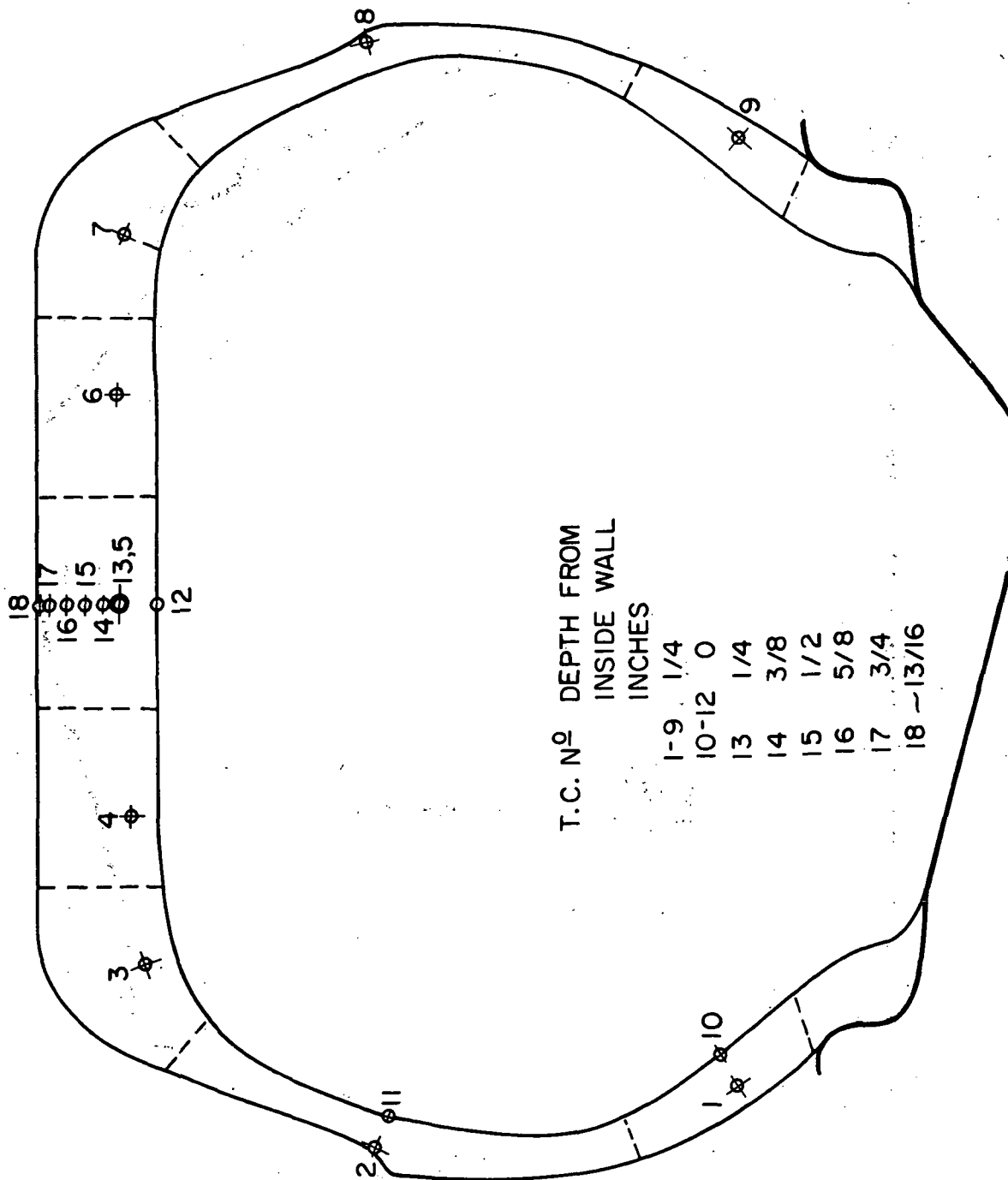


Figure 1. Thermocouple locations relative to cross section for G78-15 #5 and #8 6JK rim.

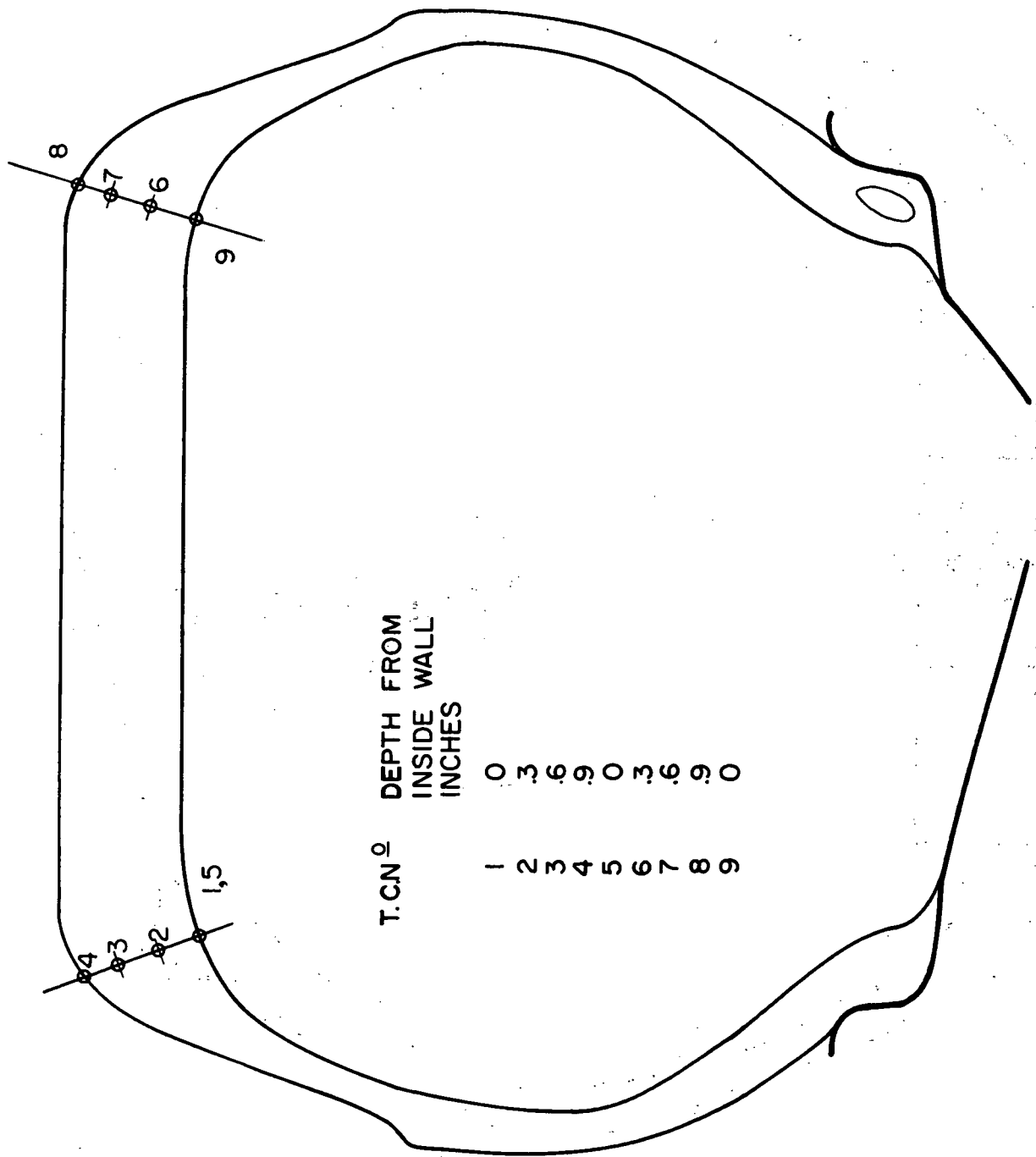


Figure 2. Thermocouple relative to cross section for H78-15 on 6JK rim (shown on a tracing of a G78-15 on a 6JK rim).

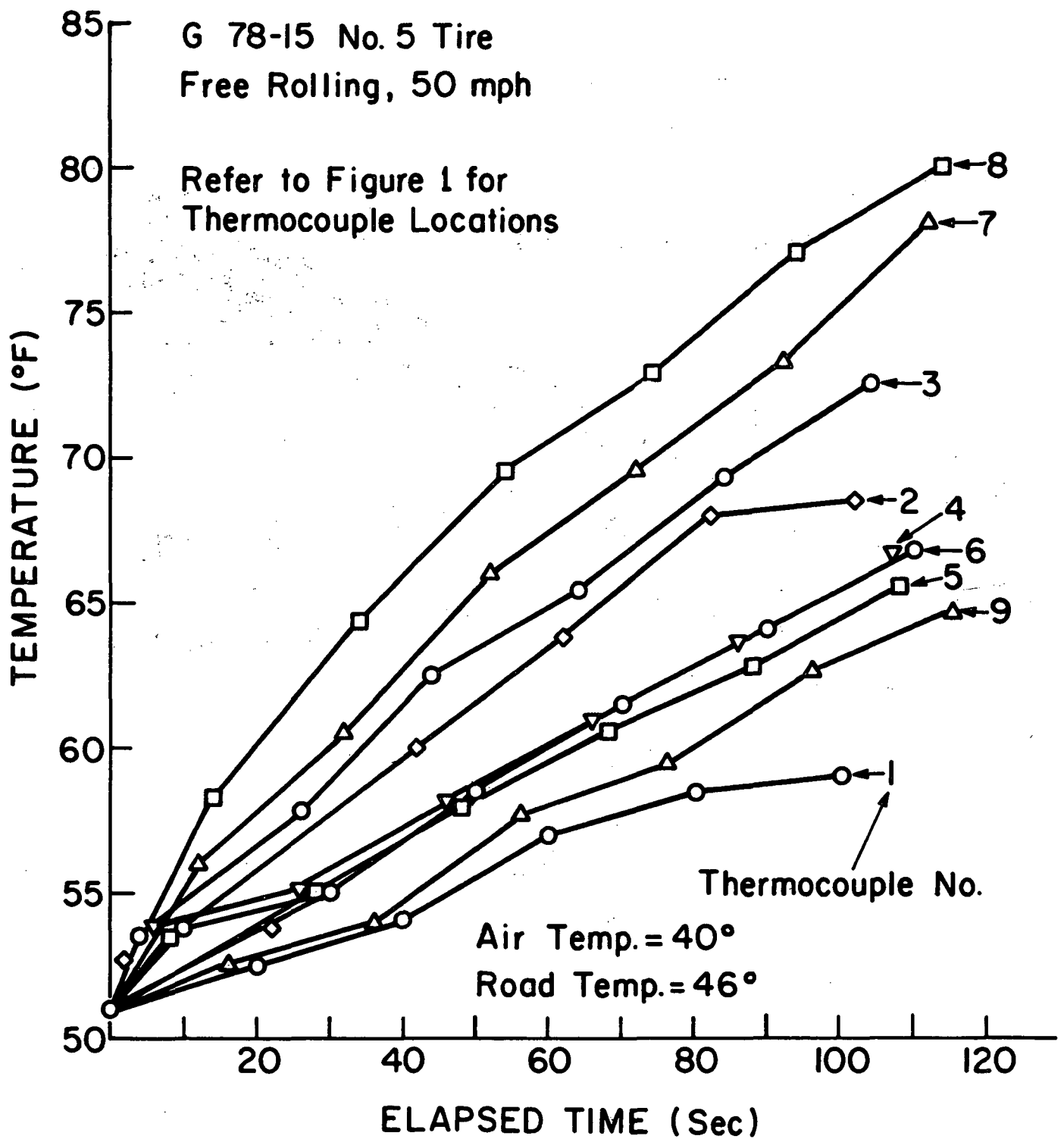


Figure 3. Temperature build-up around cross section.

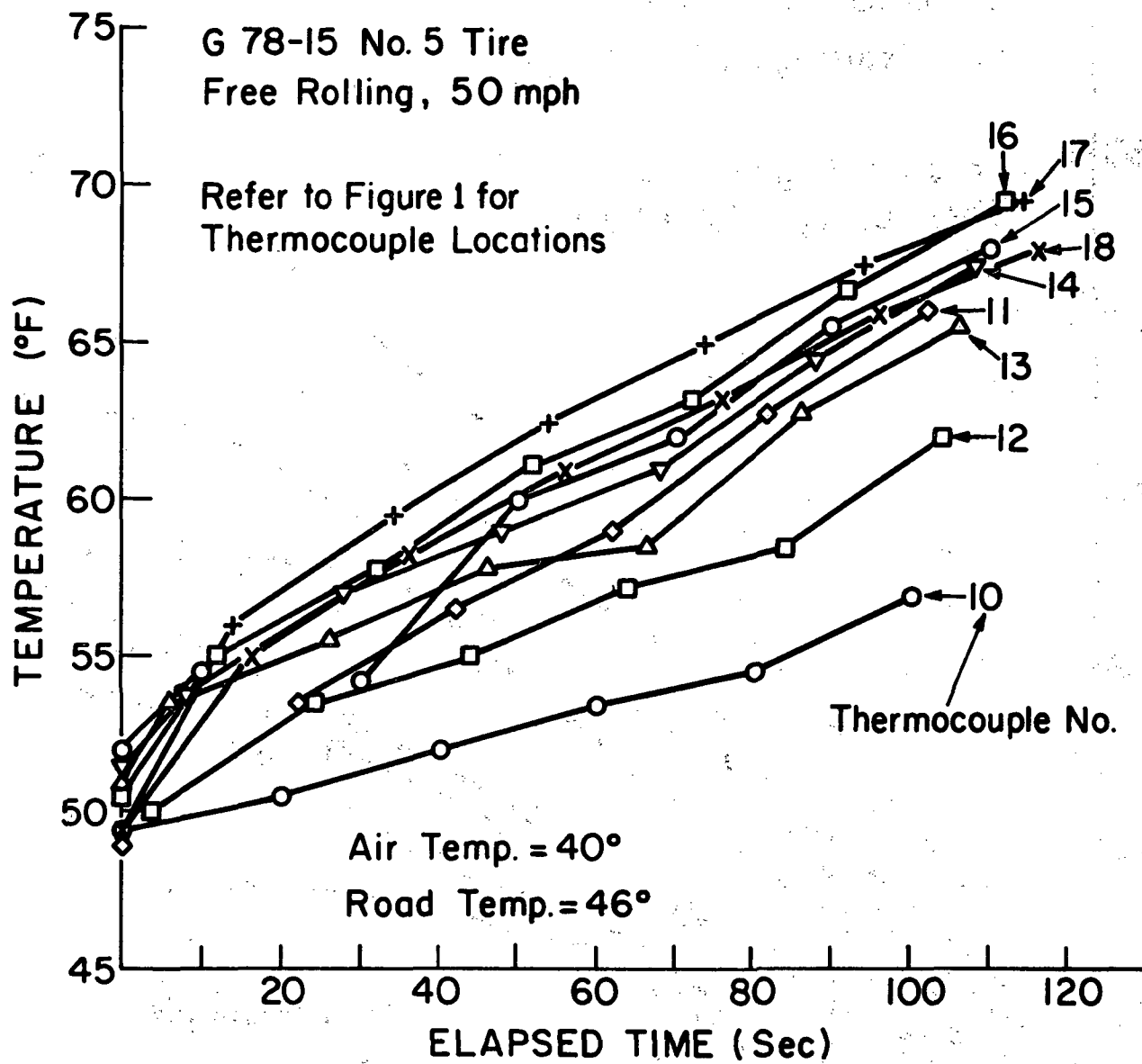


Figure 4. Temperature build-up within crown.

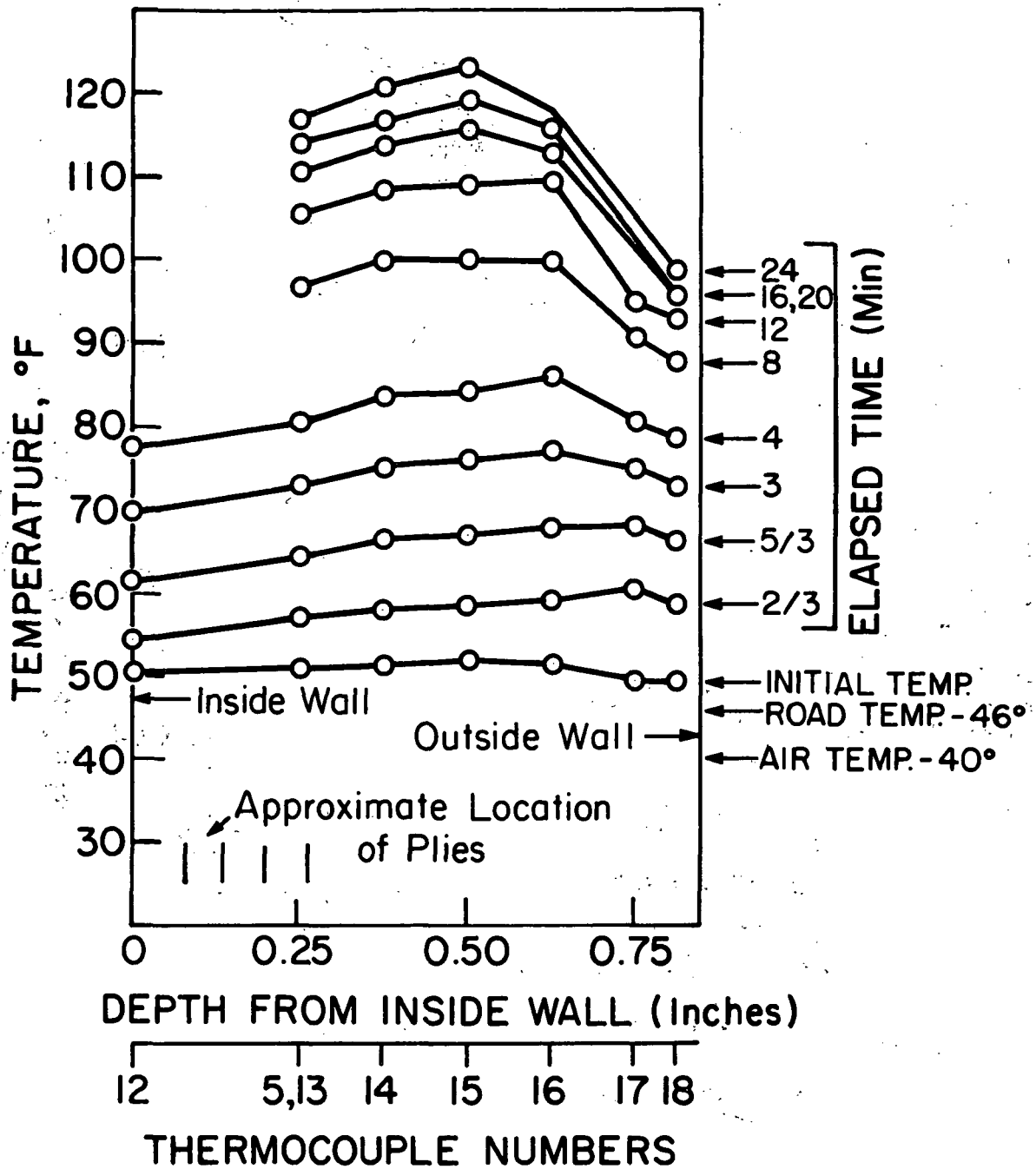


Figure 5. Temperature profiles at crown.

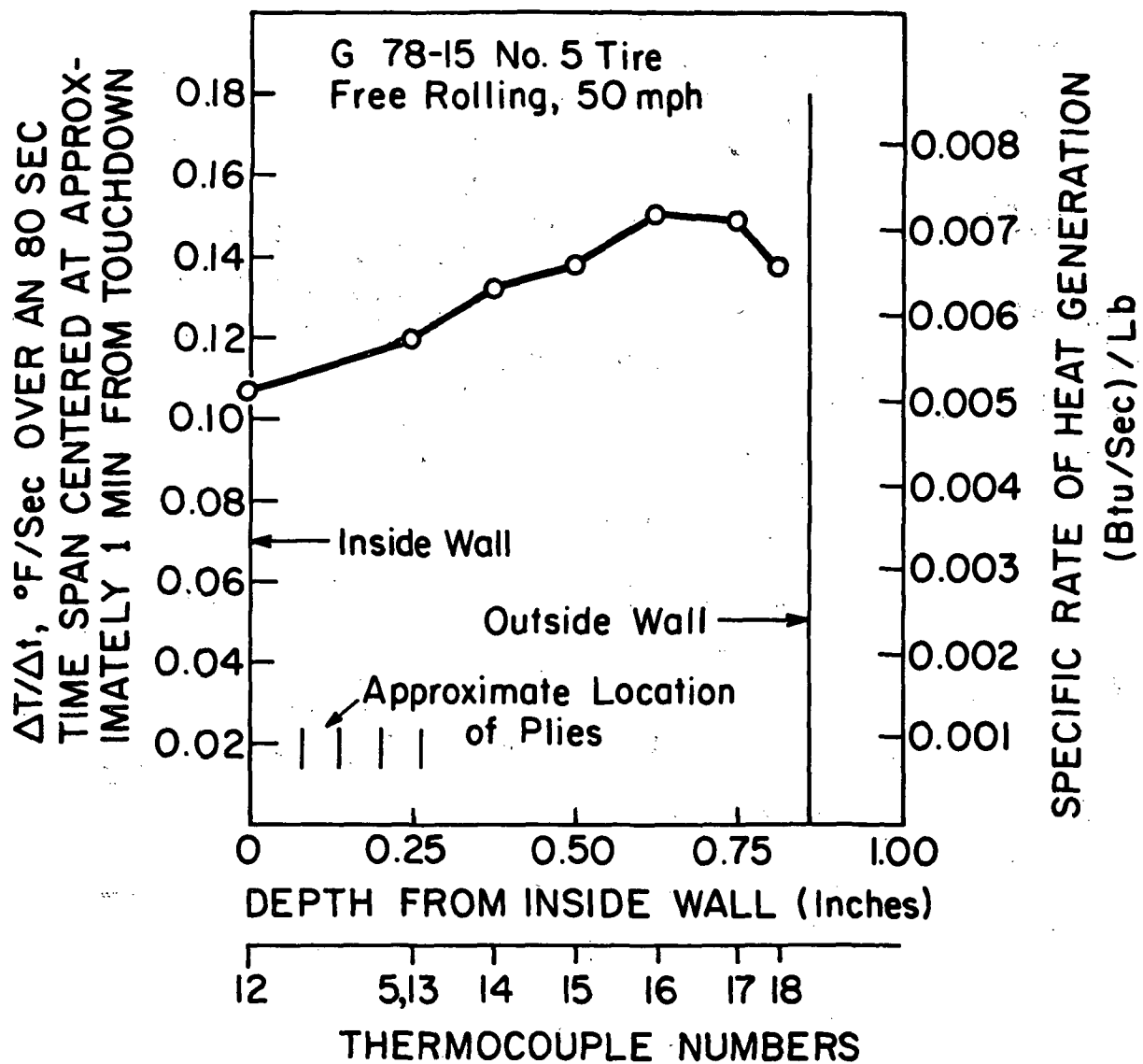


Figure 6. Heat generation profile at crown.

IV. TEMPERATURE SENSOR MEASUREMENTS

An experimental system was designed to measure the heat generation caused by the scrubbing of the tire. The term scrubbing, as used here, refers to the horizontal motions that take place within the contact patch of the tire, which contribute to the energy dissipation of the tire and which are important in the heat balance near the surface of the tire. These motions between the tire and the road result in a heat flux, due to friction, which is partitioned between the tire and the road. These motions are typically small in a free rolling, unyawed tire compared with the size of the contact patch; average values of .02 in were found in the scratch plate experiments described subsequently in this report.

The experimental system consisted of temperature sensors bonded to the road surface and an electronic system to measure and record the temperature during the brief time of contact between a sensor and a tire rolling over it at normal highway speeds.

The sensors used were thin-film temperature sensitive nickel grids bonded in a sandwich construction between two thin layers of polyimide. The construction of a sensor is illustrated in Fig. 7. The values of thicknesses shown in that figure are manufacturer's values and were not measured or checked by us. The overall size of the grid was .125 in x .125 in. Previous experience with the sensors indicated that the static temperature sensitivity was very uniform from sensor to sensor and within 1% of the manufacturer's specifications. Neither a static nor a dynamic temperature calibration was made and the manufacturer's specifications were used.

The sensors were mounted to the road using the following technique. The road surface was smoothed using sandpaper until a flat, uniform satin-like surface was achieved. Then epoxy cement was smeared into and over this region. After the cement had set it was sanded smooth and the sensors were bonded to this epoxy surface using a thin layer of epoxy cement. The surface to which the sensors were bonded was entirely epoxy with no asperities showing through. The road to which the sensors were bonded was an asphalt taxi way at Willow Run Airport, Ypsilanti, Michigan. Fig. 8 shows a sensor mounted on the road and also shows the size of the aggregate in the asphalt. Four sensors were placed in the array shown in Fig. 9 on 2.50 in centers on a line perpendicular to the path of the tire and were numbered 1-4 from right to left.

The sensors were judged to be insensitive to static strain levels resulting from a pressure of the same order of magnitude as the mean contact patch pressure. This was determined by a simple test in which a piece of rubber was laid on the sensor and the system was allowed to reach thermal equilibrium, after which a force judged to provide approximately 10 to 40 psi net, mean pressure was applied. No significant signal was observed. A lateral force applied under the conditions of normal loading described above produced no significant signal up to the point at which slipping took place. The sensors were individually incorporated into bridge circuits which also served to compensate for the slightly non-linear characteristics of the nickel grid. The overall sensitivity of the system was $0.77 \text{ mv}/^{\circ}\text{F}$, and response non-linearities were estimated to be inconsequentially small over the range of temperatures recorded.

The electrical signals produced by changes in sensor temperatures were measured using a two channel, high gain storage oscilloscope, and the traces recorded on the oscilloscope were photographed. The oscilloscope trace commenced at an external trigger signal supplied by the trigger mechanism visible near the end of the scale in Fig. 9. A subsequent test of the time response of the system showed that the electronic components and the readout technique were capable of resolving details on a time scale much less than the duration of contact.

A G78-15 patternless tire was used at 24 psi inflation pressure and 1000 lb vertical load. The tire is described in greater detail in part III of this report. The tire had, under the conditions described above, a static contact patch length on the centerline of 5.5 in and a gross contact area of 29.6 in.². This yields a mean contact pressure of 33.8 psi which is significantly higher than the inflation pressure probably because of the stiffness of the patternless tread. The tire was mounted on the Highway Safety Research Institute Mobile Tire Tester as shown in Fig. 10. This piece of equipment, which will be referred to as the truck, was equipped with a yoke on which the tire was mounted, and which could be raised and lowered rapidly. The truck was also equipped with a system for measuring and recording the forces acting on the tire. Because the small drag forces associated with free rolling, unyawed operation were smaller than the resolution of the system, no drag records were made.

A heat flux can be caused by the conductive flow of heat between the tire and the road due to a temperature difference between the tire surface and the road surface, as well as by scrubbing, so that

it was necessary to either minimize this source of flux or to separate the net flux into conductive and scrubbing components in order to isolate the flux due to scrubbing. For this reason two types of experiments were conducted. The first was done in such a way as to minimize the conductive heat flux, by operating with the tire surface temperature and the road surface temperature as close to one another as feasible. In this type of experiment the truck approached the sensor array at 50 mph with the tire held off the pavement by raising the yoke. At a distance of approximately 100 ft up track of the sensor array the tire was released suddenly. After a few bounces the tire rolled smoothly and if the trigger was contacted, indicating that the tire had passed over the array, the signal stored on the oscilloscope was recorded photographically. The precise path of the tire was recorded by a device located down the track from the array. It was found early in the testing program that it was impossible to control the lateral path of the truck with any degree of precision, so that on some trials the tire did not pass over the sensor array properly or else missed it altogether.

The purpose of releasing the tire very close to the sensors was to minimize tire heating and to provide a tire temperature close to the road temperature. The approximately 100 ft of tire-road contact would yield approximately 14 revolutions of the tire before contact with the sensors, so that the area which did contact the sensors had suffered approximately 14 contact episodes with the asphalt pavement before reaching the polyimide sensor surface. It appeared from the nature of the signals recorded that the surface of the tire did not

heat appreciably during the run over the pavement. It should be noted that some uncertainty was introduced by this technique because some part of the circumference of the tire was involved in accelerating the tire rotationally. That is, the friction on some part of the tire must have been large in order to spin the tire up to speed. The location of this area, which was the original contact patch, was not known absolutely nor was it known relative to the area of the tire which contacted the sensors.

The results of an experiment of this type are illustrated by a copy of the data sheet for trial 6, July 27, 1971.

The sensor was very sensitive, as can be judged by the oscilloscope sensitivity used, and the signals which were recorded were very small. For example, it was necessary to run these tests before the sun had risen because clouds passing in front of the sun caused temperature fluctuations large enough to drive the signal beyond the range of the oscilloscope. The sensors were also sensitive enough to respond to turbulent air fluctuations caused by placing an obstacle, say 2 ft square, a few feet upstream of the sensors in the early morning breeze. The approximate duration of contact, as calculated from the static contact patch length and the forward velocity, was 6.25 msec which is approximately 3 cm on the oscilloscope screen.

A second type of experiment which produced a significantly greater temperature signal was also conducted. In this case the tire was run approximately 1 mile on the pavement in a straight line before passing over the sensors. The tread surface of the tire was consequently significantly warmer than the sensor or pavement surface

DATA FORM 036390

TRIAL NO. 6

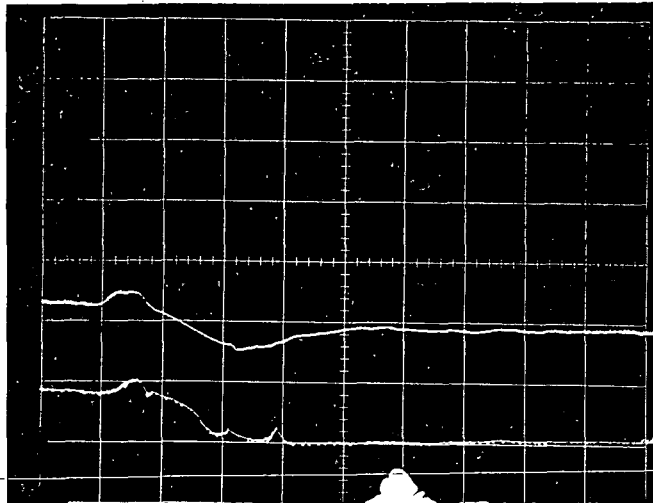
July 27, 1971

OVERALL
SENSITIVITY

.26 °F/cm

SENSOR # 2

SENSOR # 3



2 ms/cm SWEEP RATE

INSTRUMENTATION: ATTEN X _____ SCOPE SENS .2 mV/cm

VELOCITY 50 mph

TIRE: I. D. G 78-15 #5

LOAD 1000 lb PRESSURE 24 psi

TEMPERATURES °F

AIR 67

ROAD 75

TIRE 74

NOTES:

All speeds so far: 50 mph

because of accumulated scrubbing and hysteresis heat. The signal from one such experiment is shown on a copy of the data sheet for trial 8, July 27, 1971.

In both types of experiments the tire surface temperature and the road surface temperature were measured using a simple contact pyrometer which was referenced against the air temperature as measured by a mercury thermometer. In both the trials used as examples in this report only sensors 2 and 3 were used, and they were used to measure relative temperatures so that the separation of the signals on the oscilloscope screen represents only a convenient spacing to facilitate measurement, and does not indicate an absolute temperature difference between the two sensors. In both trials the upper signal corresponds to sensor 2 as suggested by the form of the data sheet. The grid of the oscilloscope screen was composed of 1 cm squares. The paths of the tire relative to the sensor array for the two trials shown here are illustrated in Fig. 11 and Fig. 12.

As a preliminary to remarks concerning the results of trials 6 and 8, the results of an analytical treatment of the sensor response are of interest. The details of the model and the solution of the pertinent equations are described in Appendix 1. Reference to that appendix will show that the form of the response as given in Eq. 5 is sufficiently complicated to warrant solution via a computer program and to justify the use of a graphical form of output. Figure 13 illustrates the response of the sensor to a unit heat flux of 6.25 msec duration as shown in Fig. 14. The response of the sensor up to 6.25 msec is the response to a unit magnitude heat flux applied as a step function

DATA FORM 036390

Duration of contact based on contact
patch length and velocity.

TRIAL NO. 8

July 27, 1971

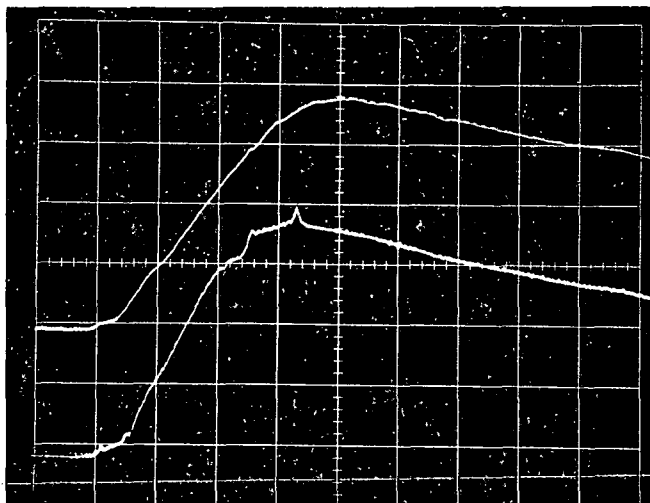


OVERALL
SENSITIVITY

.26 °F/cm

SENSOR # 2

SENSOR # 3



2 ms/cm SWEEP RATE

INSTRUMENTATION ATTEN X SCOPE SENS .2 mV/cm

VELOCITY 50 mph

TIRE: I. D. 678-15 # 5

LOAD 1000 lb PRESSURE 24 psi

TEMPERATURES °F

AIR 69, 68 at bench

ROAD 77

TIRE 84

NOTES:

Tire down for approximately 1 mile of
continuous running prior to contact.

to the surface of the sensor. The initial response of the sensor is instantaneous but very small and the time delay is only apparent, not real. The maximum of the response shown in Fig.13 is 6.22×10^{-4} °F ft² hr/BTU and occurs at approximately 6.5 msec. It should be noted that this model is sensitive only to a net heat flux and cannot discriminate between interfacially generated heat, which is partitioned into a flux into the tire and a flux into the sensor, and a heat flux across the interface due to the conductive exchange of heat between the tire at one temperature and the sensor at another. To discriminate between these fluxes would require a knowledge of the contact resistance which we do not have and cannot determine using the simple model.

The two types of signals recorded correspond to the two types of experiments conducted. In the first type, the smallest net conductive heat flux possible under the experimental conditions is superimposed on the heat flux due to scrubbing, although we cannot tell how much each contributes to the sum. In the second type the heat flux due to conduction is much larger because it represents accumulated heat, and is presumably larger than the heat flux due to scrubbing. However, in neither case is it possible to isolate the contribution due to scrubbing using the model and the analytical tools at our disposal, although some observations about the gross nature of the results can be made and explanations offered with some degree of confidence.

In trial 6 the tire was slightly cooler than the road and had rolled only about 100 ft so that a decrease in temperature during contact might be anticipated and indeed this seems to be the situation. However, the seemingly erratic nature of the signals during contact

defies our analysis and suggests a flow of heat into and out of the sensor which we cannot explain in detail. Furthermore, no explanation can be offered as to why the signals in that trial indicate a temperature drop of approximately $.1^{\circ}$ F and $.2^{\circ}$ F but did not rise appreciably toward their initial values in the 12 msec following contact. On the other hand the signals in trial 8 show a decided downward trend toward their initial values almost immediately after contact ceased. The spike that appears in the signal for sensor 3 near the end of contact remains an enigma. Spikes of this type appeared in several trials, most often near the end of contact, and trial 8 contains a similar spike. The only speculation that can be offered is that it represents a stick-slip phenomenon that occurs in the trailing edge of the contact patch.

In trial 8 the tire was significantly warmer than the road and the sensor response resembles the response of the model to a heat flux pulse of constant amplitude and 6.25 msec duration, in so far as the overall shape is concerned. However, the recorded signals have minor variations in slope which may contain information but which cannot be analyzed with the model used. The response of sensor 3 near the end of contact and the final spike remain to be explained. The only conclusion that can be drawn is that a conductive heat flux of approximately constant magnitude existed during the time of contact and that some interfacially generated heat caused by scrubbing was superimposed upon this conductive flux, but nothing can be said about the form of the flux using this approach.

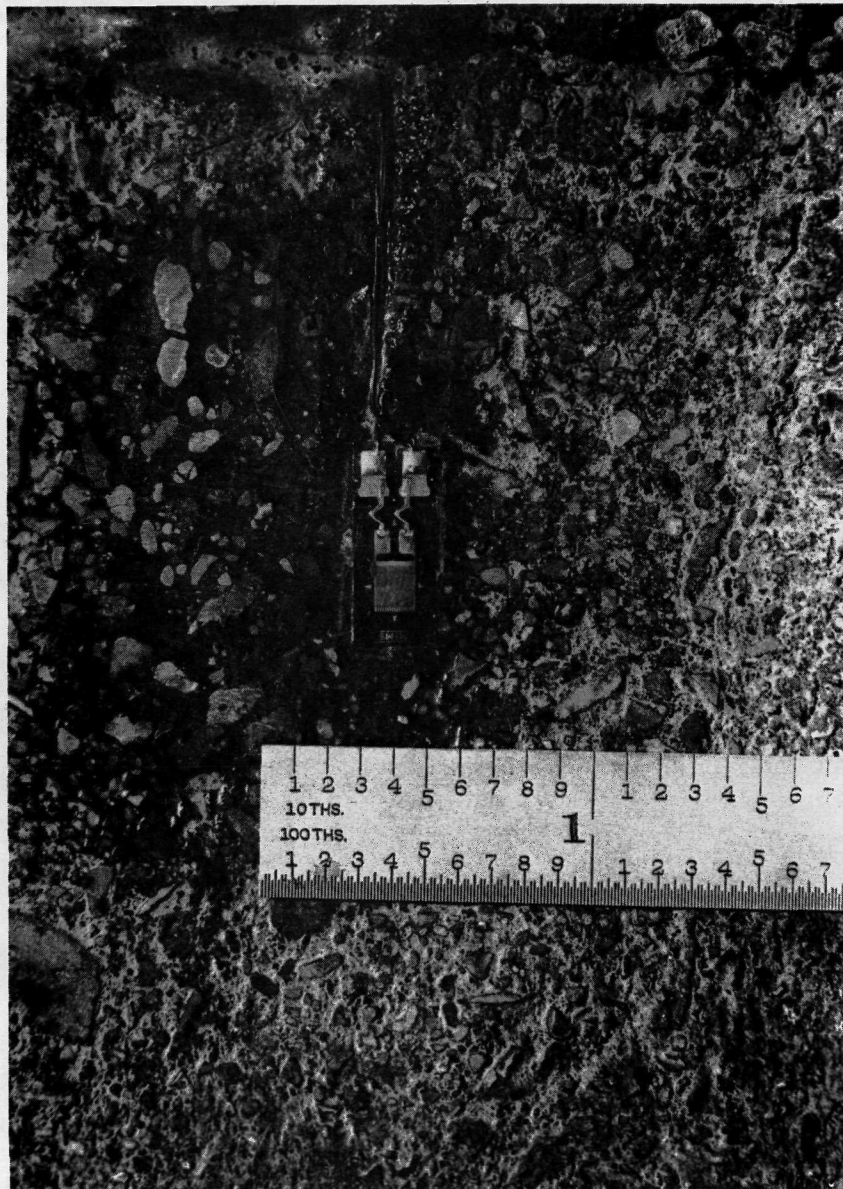
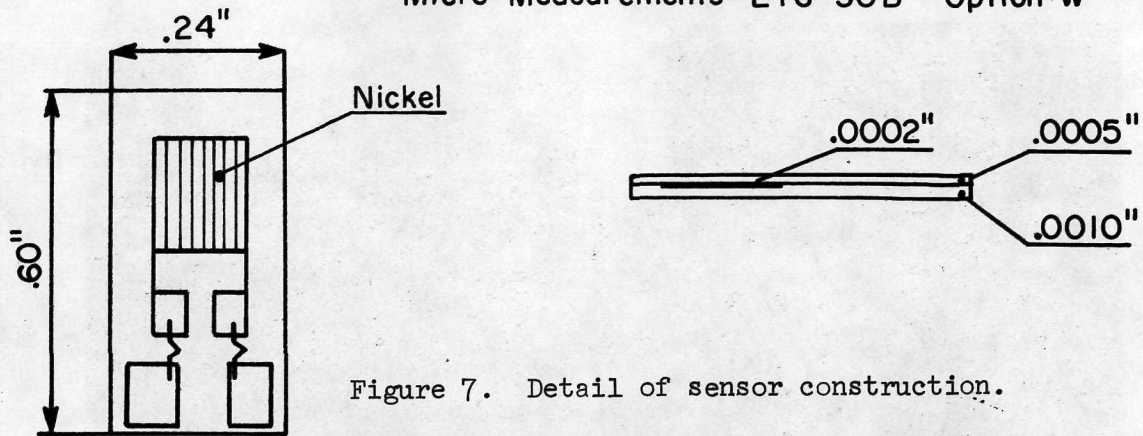


Figure 8. Sensor mounted on pavement.

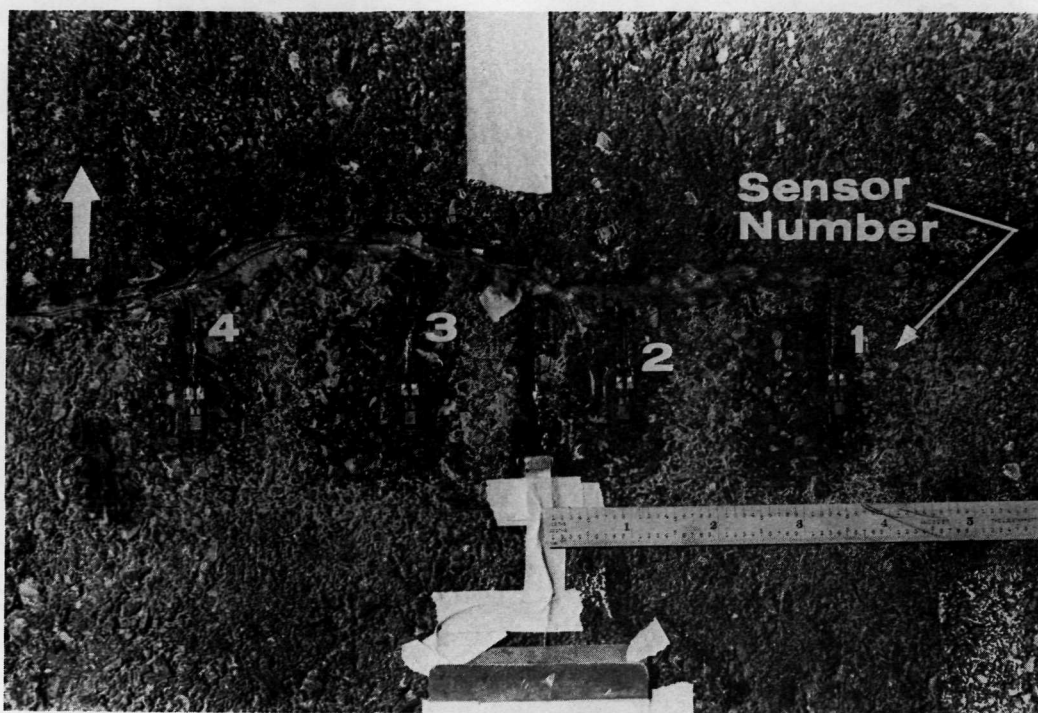


Figure 9. Sensor array on pavement



Figure 10. Treadless test tire mounted on truck.

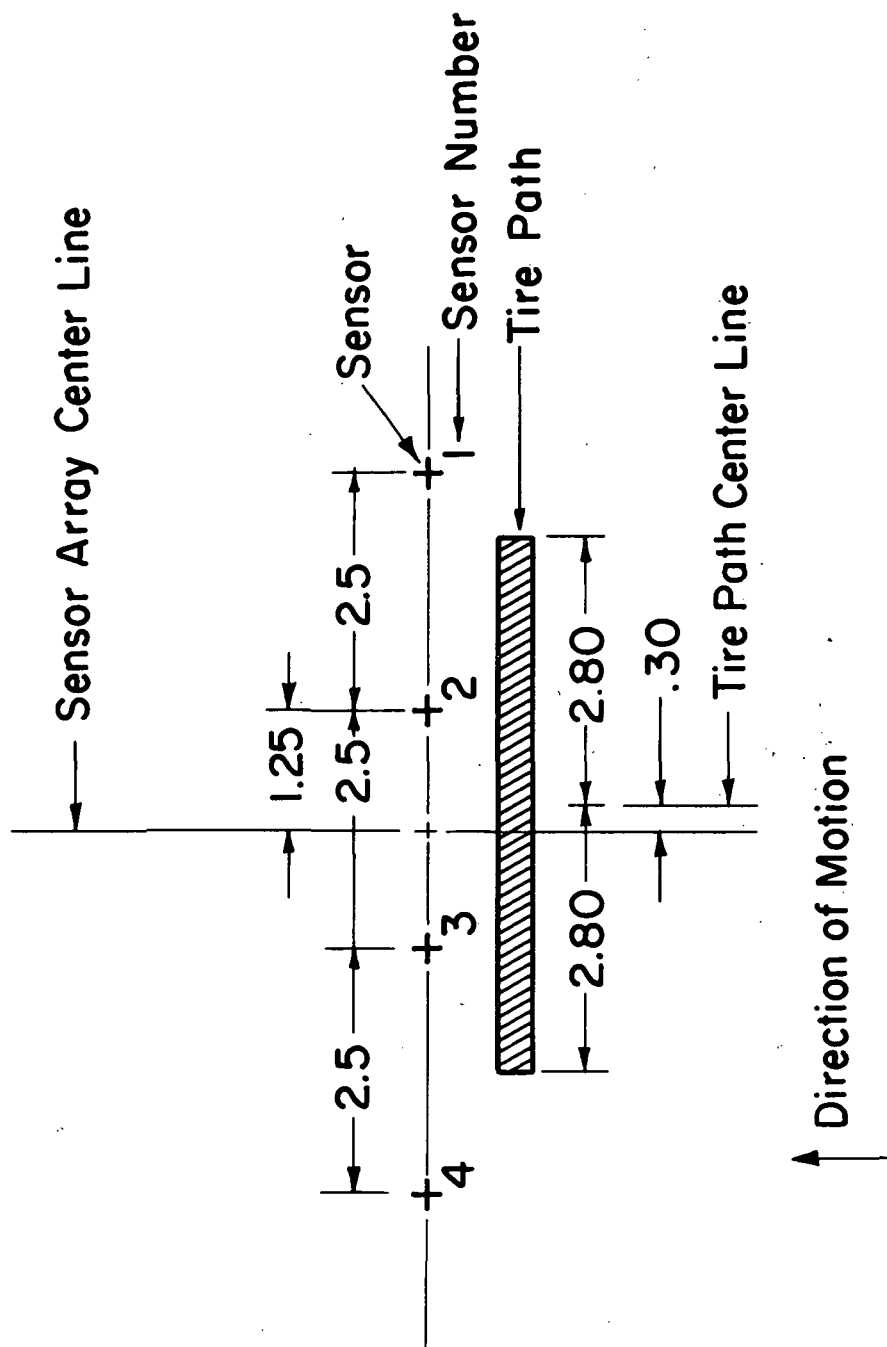


Figure 11. Tire path record for Trial 6. All dimensions in inches.

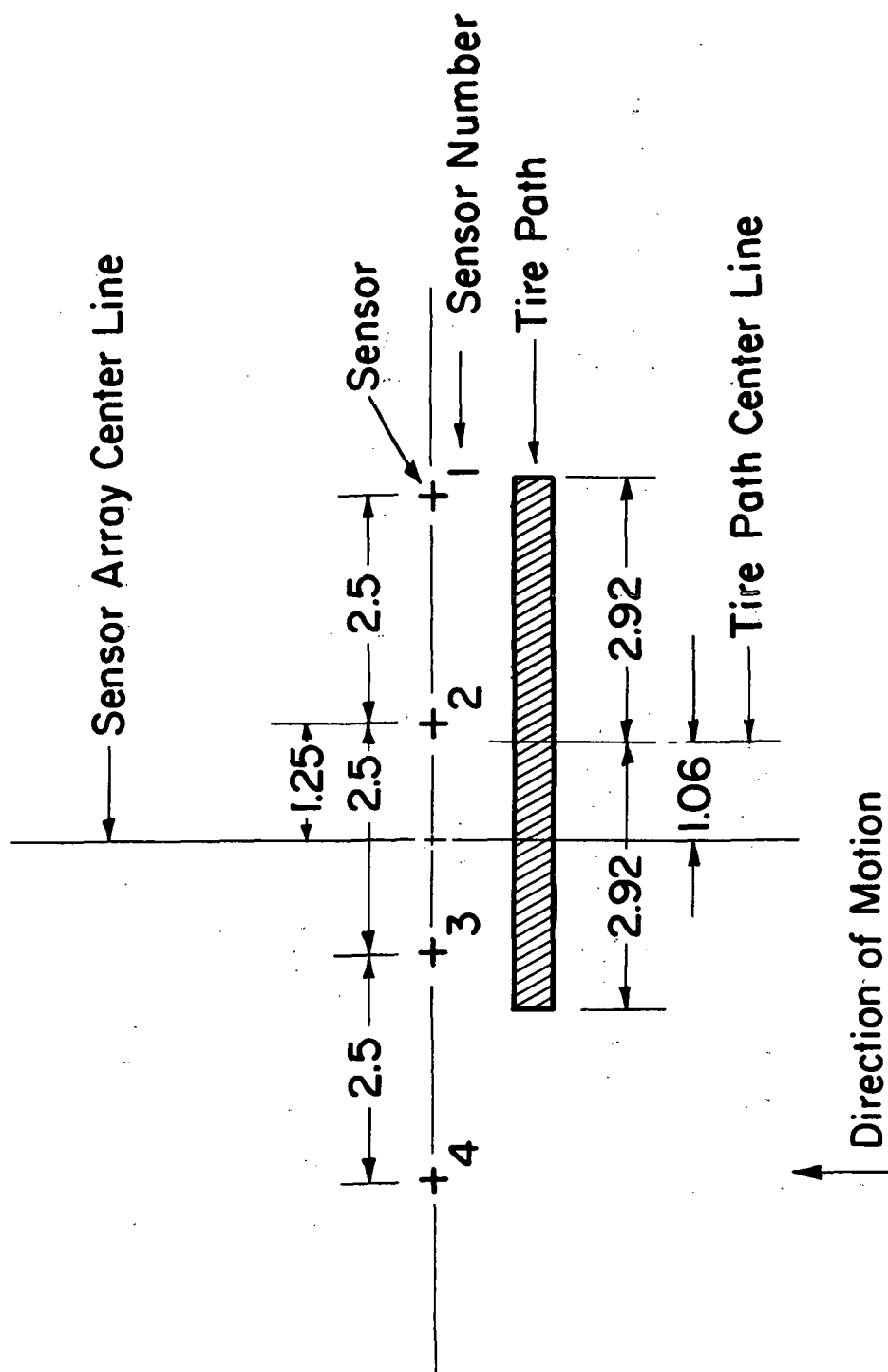


Figure 12. Tire path record for Trial 8. All dimensions in inches.

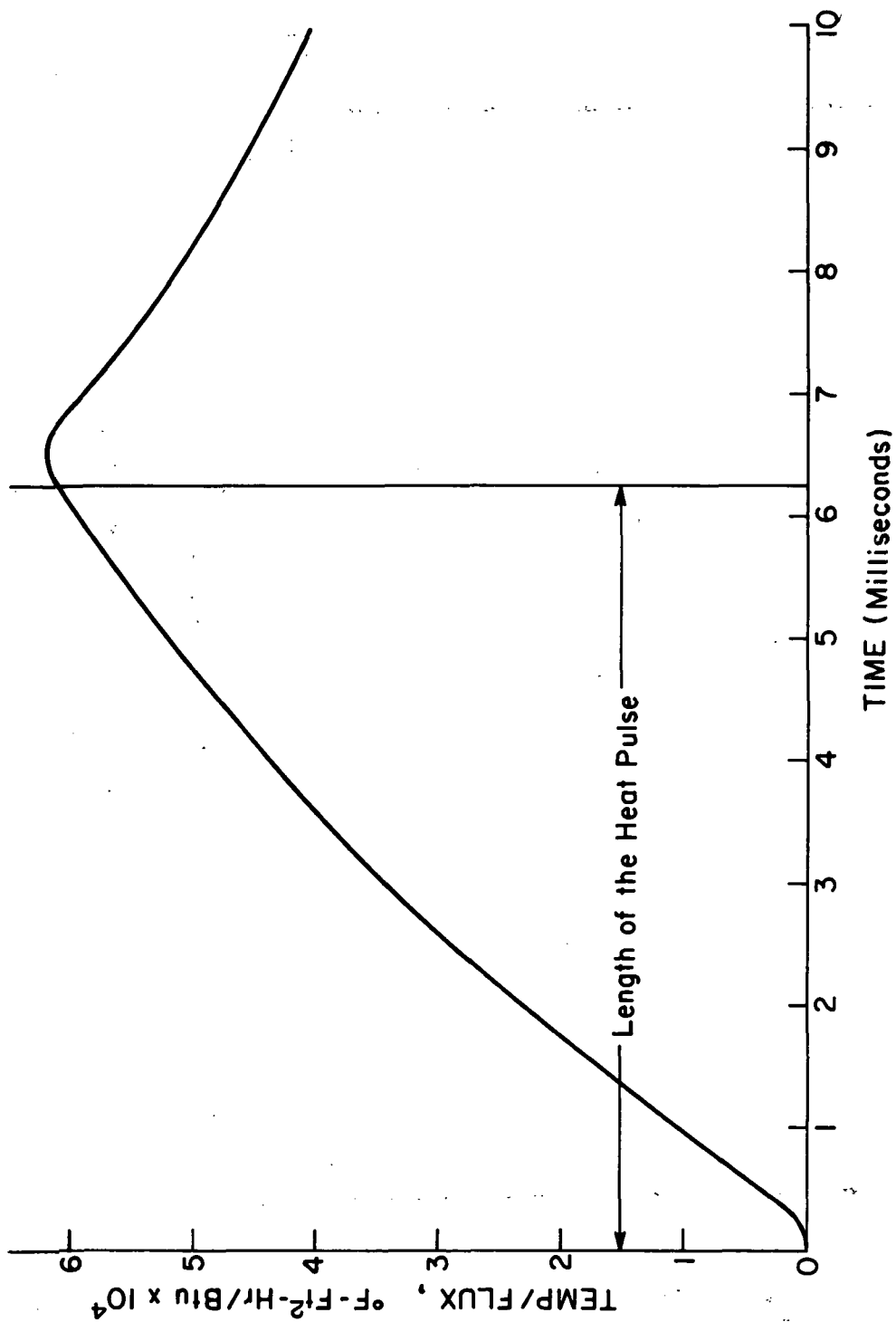


Figure 13. The response of the sensor to a heat flux pulse.

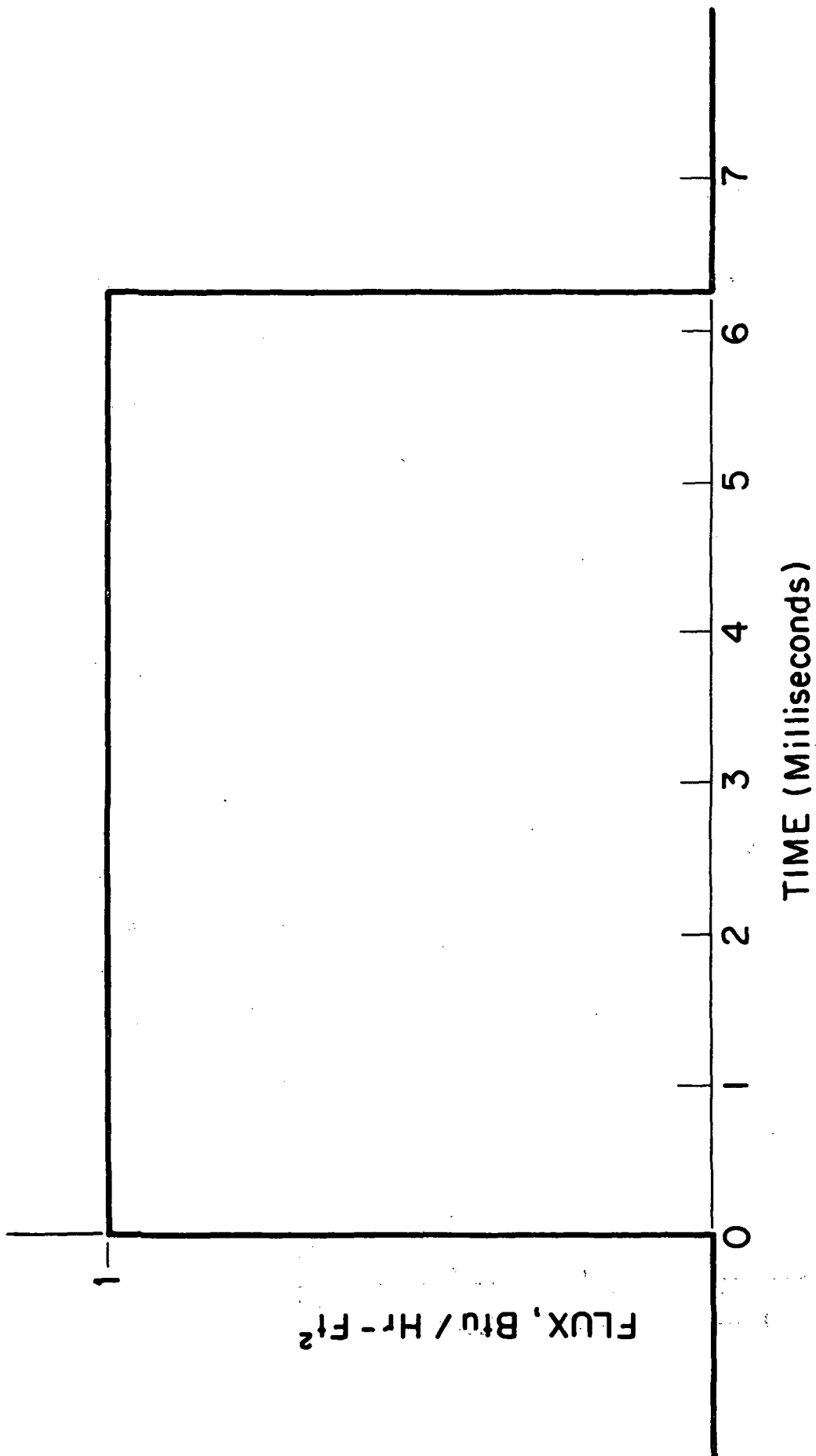


Figure 14. Heat flux pulse of constant unit magnitude.

V. SCRATCH PLATE MEASUREMENTS

One relatively simple mechanical method for measuring the energy losses at the surface of a rolling tire is to cause the loaded tire to roll over a smooth metallic plate upon which carborundum particles have been sprinkled. The grit embeds itself in the tread rubber and causes scratch marks on the plate surface as the grit particles pass through the tire contact patch. These scratch marks are indications of the amount of surface scrubbing present in the tire contact patch area.

It is difficult to assess the accuracy of this method. Insofar as is known there is no study presently available comparing the measured deflections obtained from scratch records with those obtained from more sophisticated instrumentation. It must be surmised that the scratch records could not, in general, be larger than the displacements undergone by the tire surface in the absence of the grit, provided that the friction coefficients between the actual road surface and the metallic plate were the same. This is because the embedding of the grit particles into the rubber surface would, in general, cause scratch records to be equal to, or smaller than, the actual distances moved. In view of the uncertainty between the actual distances and the resulting scratch records, and the additional uncertainties concerning equality of the friction coefficient between a real roadway and a metallic plate, these scratch records can only be used as an indication. However due to the possibility of relative motion between grit particles and the tire tread, it is probable that the tire actually experiences more scrubbing than is indicated by this study.

In the specific work reported here, 8.25 x 14 size bias belted passenger tires furnished without tread pattern by the B. F. Goodrich Tire Company were used on The University of Michigan Highway Safety Research Institute flat plank tire testing machine in order to produce such scratch records. The plates used were .005-in. brass, and the grit material was carborundum. The load on the tires was 1000 lb at an inflation pressure of 24 psi. These are standard conditions which have been used on these same tires for other tests.

The tires were rolled in straight line, nonbraking, fashion over the scratch plates in three separate tests. The scratch plates were observed under a medium power microscope and the lengths of the resulting scratches were measured. These lengths were averaged over the width of the contact area and the total length of a scratch, on the average, was found to be 0.02 in.

Assuming a pressure distribution equal to the inflation pressure of 24 psi, assuming a contact patch width of 6 in., and further assuming a friction coefficient between the tire and brass plate of 0.8, a total drag force associated with these tires, due to surface scratching alone, can be computed. This gives a value of drag force due to surface scrubbing ≈ 2.0 lb.

In view of the fact that other measurements indicate that the total drag force associated with these tires at slow speeds is at least 20 lb, then one must conclude from these scratch records that the surface effects cause a contribution to the total energy loss in the neighborhood of 10% or more of the total. This implies that only a small portion of the total losses can be ascribed to surface scrubbing directly, at least at these low speeds.

VI. MODEL TIRE STUDIES

Two basic types of experiments were carried out on a 4.5 in. diameter tire, scaled down from a Type VII 40 x 12-14 PR aircraft tire. The tire model and its construction are described in Ref. [3]. One experiment was to measure the drag force of the free-rolling tire, while the other experiment was to measure the surface temperature of the free rolling tire. Both experiments were performed on a 30 in. diameter road wheel using two different surfaces of contact for the tire. One surface was the cast iron of the road wheel itself, while the other surface was Safety Walk.* In a separate experiment these two surfaces exhibited similar static coefficients of friction. However, since the Safety Walk is made up of abrasive sand grains bonded by a glue to cloth backing, it is clear that their thermal properties are quite different. No formal attempt was made, however, to measure the thermal characteristics of the Safety Walk.

Drag-force measurements were made on the freely rolling tire by use of small force transducers located in the axle between the tire and its supporting yoke. At the same time the side force perpendicular to the wheel plane was measured as a function of yaw angle. Bearing drag was estimated and subtracted from the drag-force measurements by use of a Plexiglas model wheel of the same size as the tire, but of essentially rigid construction and with extremely low loss characteristics. By subtracting this bearing drag component, the actual tire drag could be obtained for any set of conditions.

* Trade Mark.

Tire surface temperatures were measured with an Ircon model CH-34L infrared radiation thermometer which had been previously calibrated for the emissivity of rubber. For these experiments, the average image size was approximately 3/16 in. in diameter so that the temperatures recorded represent averages over that area of the tire. Although a single individual operated this instrument throughout most of the experiments reported here, several people made check measurements from time-to-time to establish that there was no gross biasing in the temperature measurements. Figure 15 shows the positions at which temperature was measured.

The procedure for recording drag forces and tire temperatures was kept constant throughout these experiments. Each test began with the tire and rim in thermal equilibrium with the laboratory. The tire was then operated at the first test speed (500 rpm) for four minutes, after which time the drag load and temperature data were recorded. The tire was then operated at the next successive speed for two minutes before the data were recorded and this procedure was repeated until the entire range of speeds had been covered. This procedure was followed for all yaw angles. A vertical load of 38 lb and an inflation pressure of 20 psi were used throughout the tests.

While considerable care was taken in measuring the steer angle values quoted in the subsequent figures, the mechanism for this was not as accurate as desired and so one must interpret the resulting yaw angle data as subject to an uncertainty of approximately $\pm 1^\circ$.

Considerable care was also taken to insure that the measurements of temperature with the two different surface coatings on the roadwheel were taken under identical yaw angle conditions. This was accomplished by setting the test tire at a particular yaw angle and carrying out the measurements of temperature on both surfaces without changing this yaw angle setting.

Figures 16, 17, and 18 are typical surface temperatures measured at the three basic positions on the tire for zero yaw angle. On all three figures, it will be noticed that for both surfaces on the roadwheel, the center tread position is the coolest, the sidewall is the hottest while the shoulder surface temperature is intermediate. As is to be expected, the temperatures and temperature differences at the three positions increase with speed. Figure 18 is particularly interesting in that it can be seen that both the center tread and shoulder positions exhibit higher temperatures while running on the Safety Walk surface than they do when running on the cast iron surface. However, the sidewall temperatures are the same for both roadwheel surfaces.

Figures 19 and 20 show the temperature change through the contact patch for the center tread and shoulder positions. Shoulder temperature is taken on the so called tension shoulder as shown in Figure 15. The tension shoulder temperature shows a definite tendency to increase on both road surfaces for both the 0° and 2° yaw angle conditions, but not for the other yaw angle conditions. There does not appear to be a great deal of speed dependence.

Unfortunately the arrangement on the experimental apparatus did not allow us to measure the temperature on the compression shoulder of the tire as it passed through the contact patch. Consequently, little can be concluded about this particular position on a yawed tire. Figure 21 shows temperature difference between the compressed shoulder and the tension shoulder at the entrance to the contact patch of a yawed tire. On both roadway surfaces the compressed shoulder is hotter than the tension shoulder in general.

Figure 22 shows the temperature difference between the compression sidewall and the tension sidewall under identical running conditions. Here, the compressed sidewall is always hotter than the tension sidewall, with little influence of roadwheel surface apparent here.

Figure 23 through 28 illustrate particular temperature levels for various positions on the tire under different yaw angles and speeds, using the two different roadwheel surfaces. In general, study of this data leads one to the following conclusions:

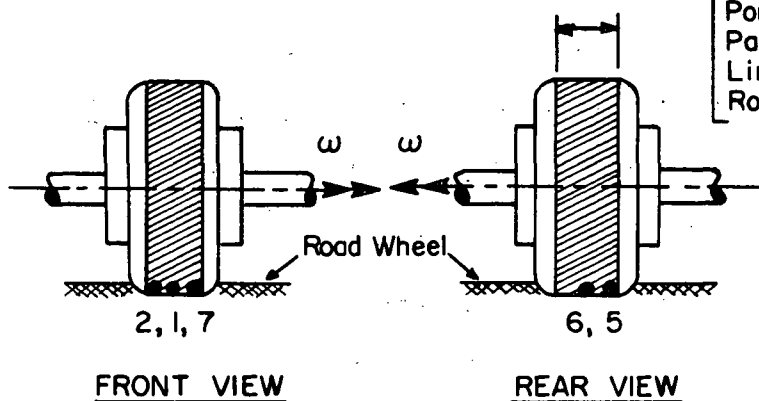
- (1) Temperatures increase in the tire with an increase in yaw angle.
- (2) Temperatures increase in the tire with an increase in speed.
- (3) Sidewall temperatures are independent of the roadwheel surface.
- (4) Points on the tire coming into contact with the road surface are hotter when run on the Safety Walk than on the cast iron.

This latter point is quite clearly demonstrated in Figure 29, which shows the difference in temperature between the two surfaces for the center tread and tension shoulder positions.

Figures 30 and 31 illustrate drag force in the wheel plane and drag force in the direction of motion, respectively, as a function of speed at several yaw angles. The nonlinearity of the data with respect to yaw angle probably indicates errors in the measurement of 0° yaw angle position, as previously mentioned. In examining this data, there appears to be little difference between drag forces measured on the Safety Walk or cast iron.

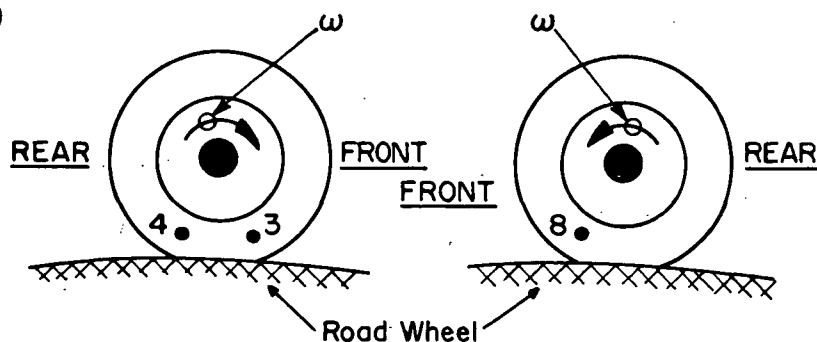
Finally it should be noted that examination of this data seems to indicate that the temperature difference between entering contact and leaving contact, as measured on the tread of the tire, is the same for the two surface materials upon which the tire was run. There appears to be evidence of a temperature rise on the surface of the tire as it passes through the contact patch at zero yaw angle, but there also appears to be evidence of a temperature drop on the tire surface as it passes through the contact area at higher yaw angles. This does not seem to clearly substantiate the theory advanced by Schallamach [4] that temperatures rise on the tire surface as it passes through the contact patch.

(a)



[Portion of Tire in Contact Patch. Excellent Demarcation Lines Could be Seen on Rolling Tire.]

(b)



Positional Data was Always Taken in the Following Sequence:
1, 2, 3, 4, 5, 6, 2, 1, 7, 8
Thus Positions 1 & 2 Gave a Fairly Good Check on Consistency of Temperature Measurements.

(c)

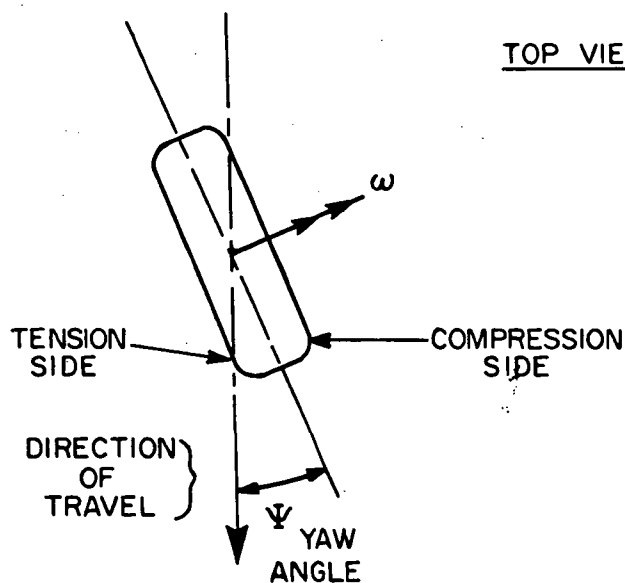


Figure 15. (a) and (b) Positional information for surface temperature measurements; (c) tire as viewed from top.

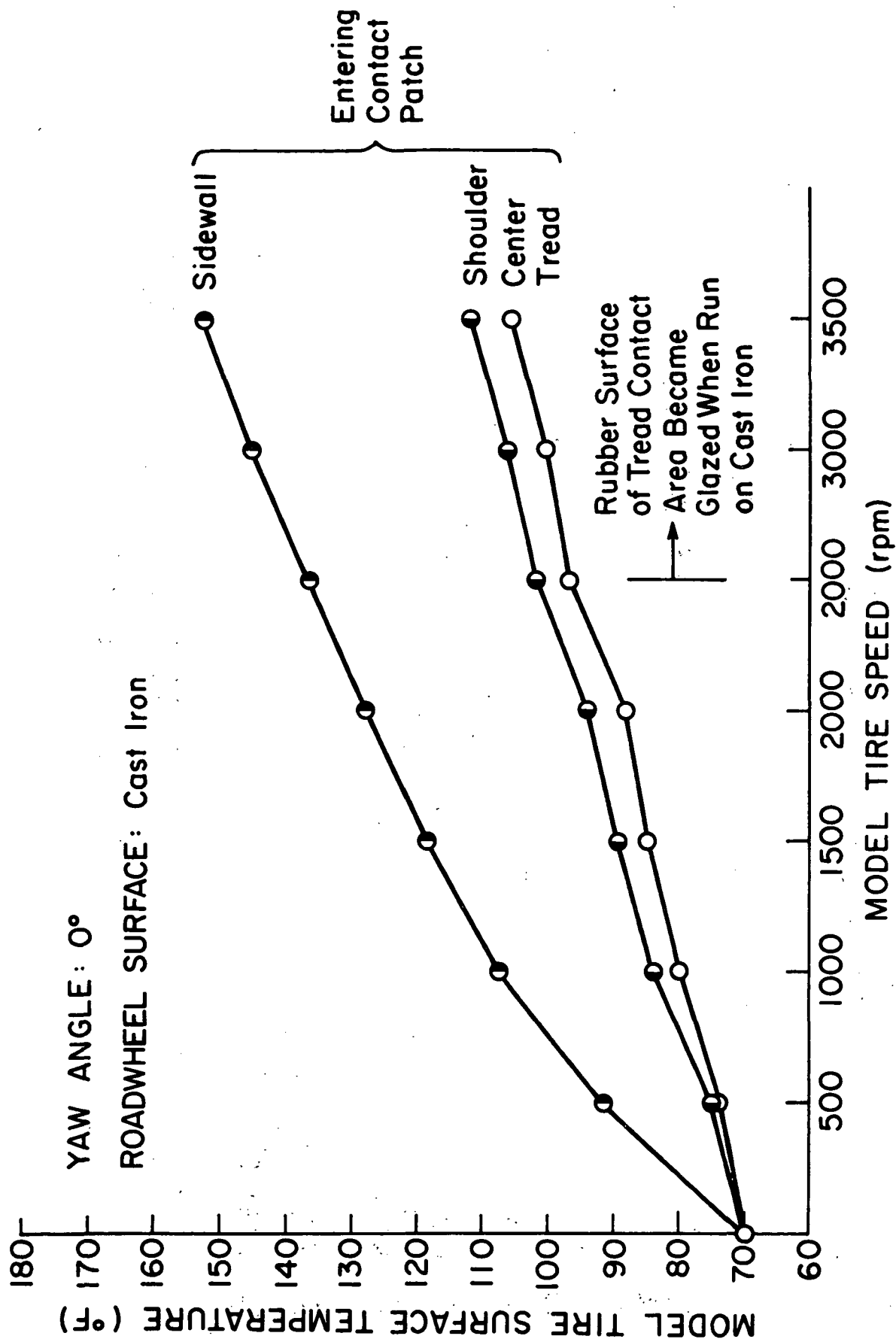


Figure 16. Surface temperatures at various positions vs. speed on cast iron at 0° yaw.

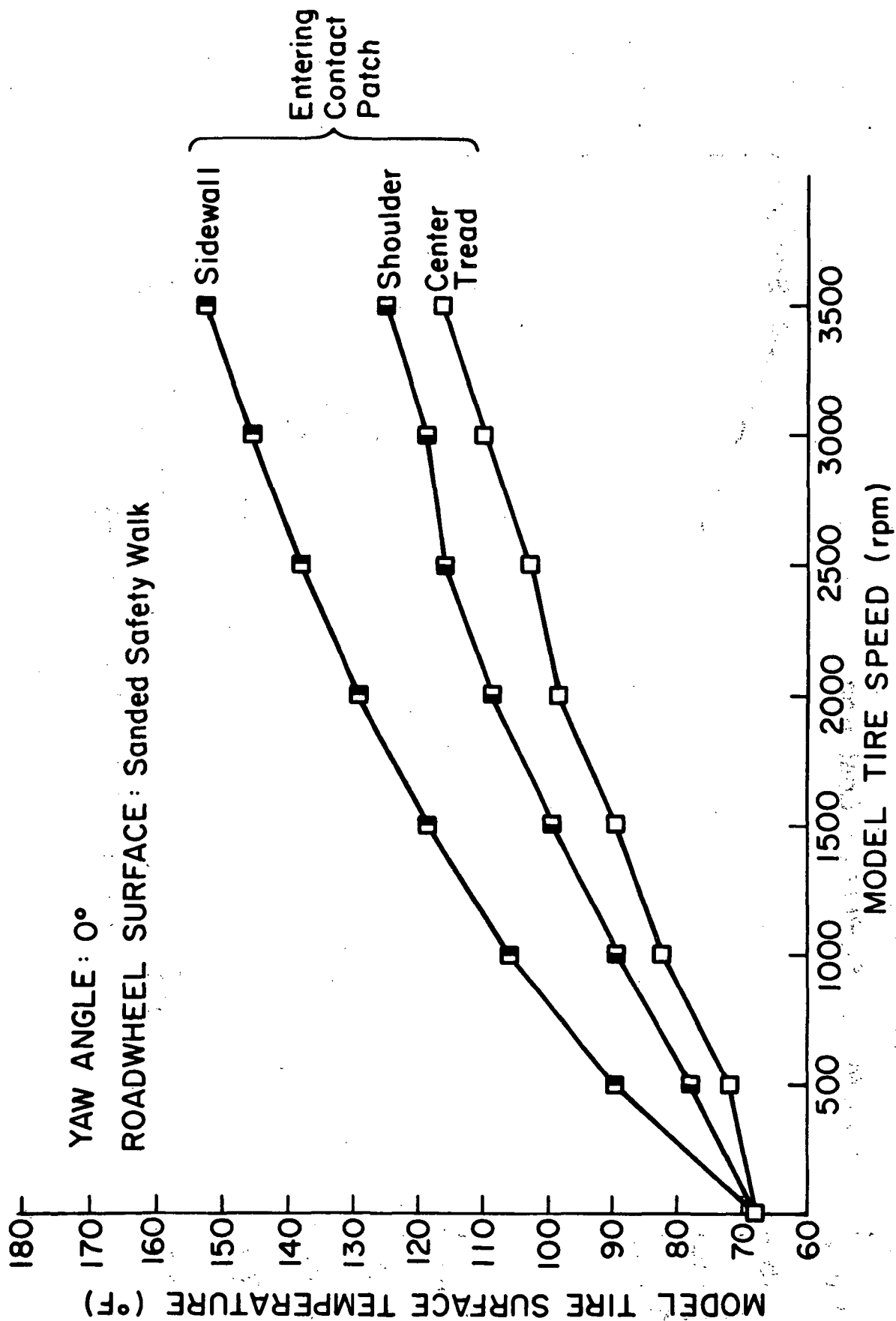


Figure 17. Surface temperatures at various positions vs. speed on sanded Safety Walk at 0° yaw.

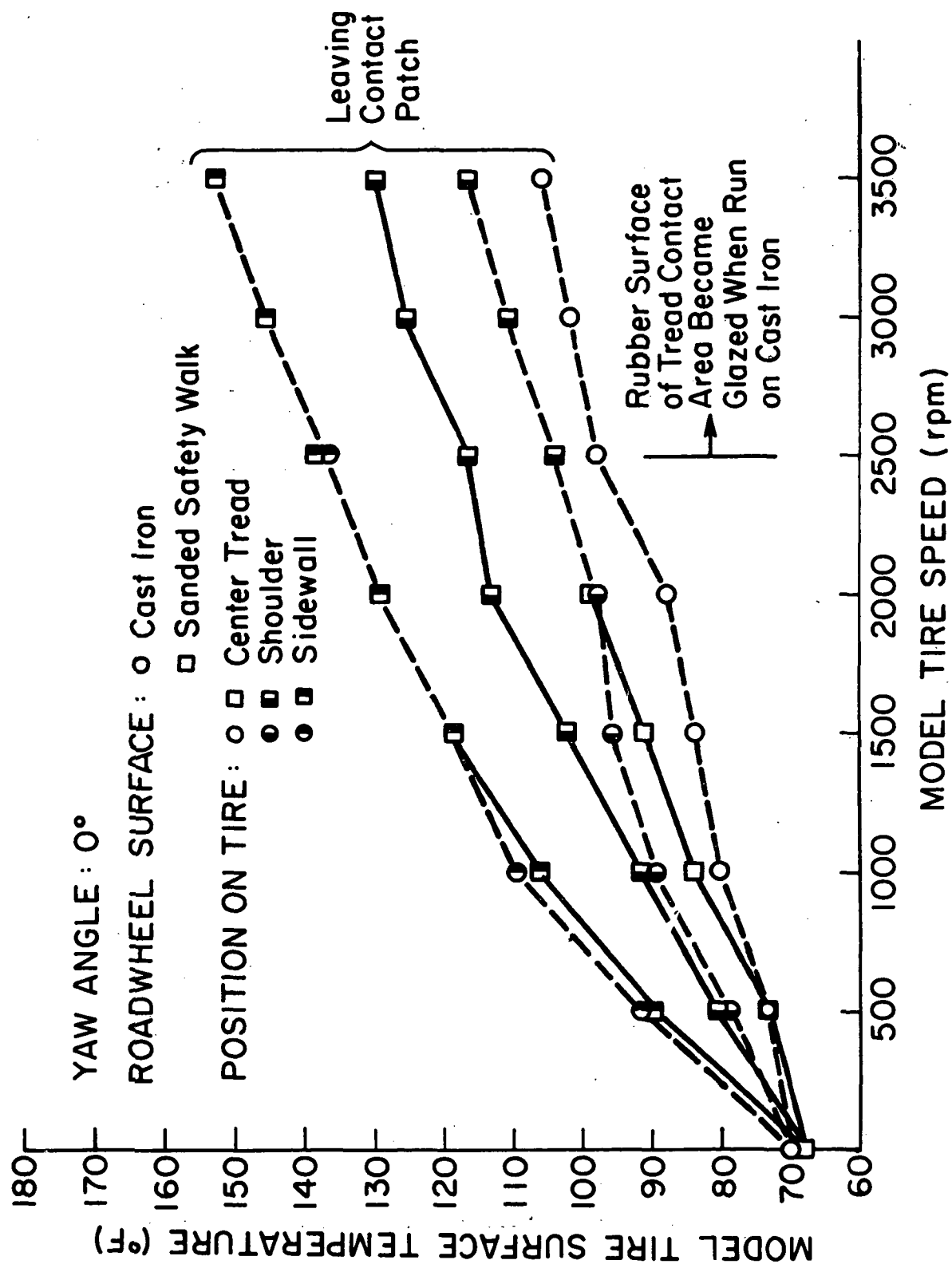


Figure 18. Surface temperatures at various positions vs. speed on iron and sanded Safety Walk at 0° yaw.

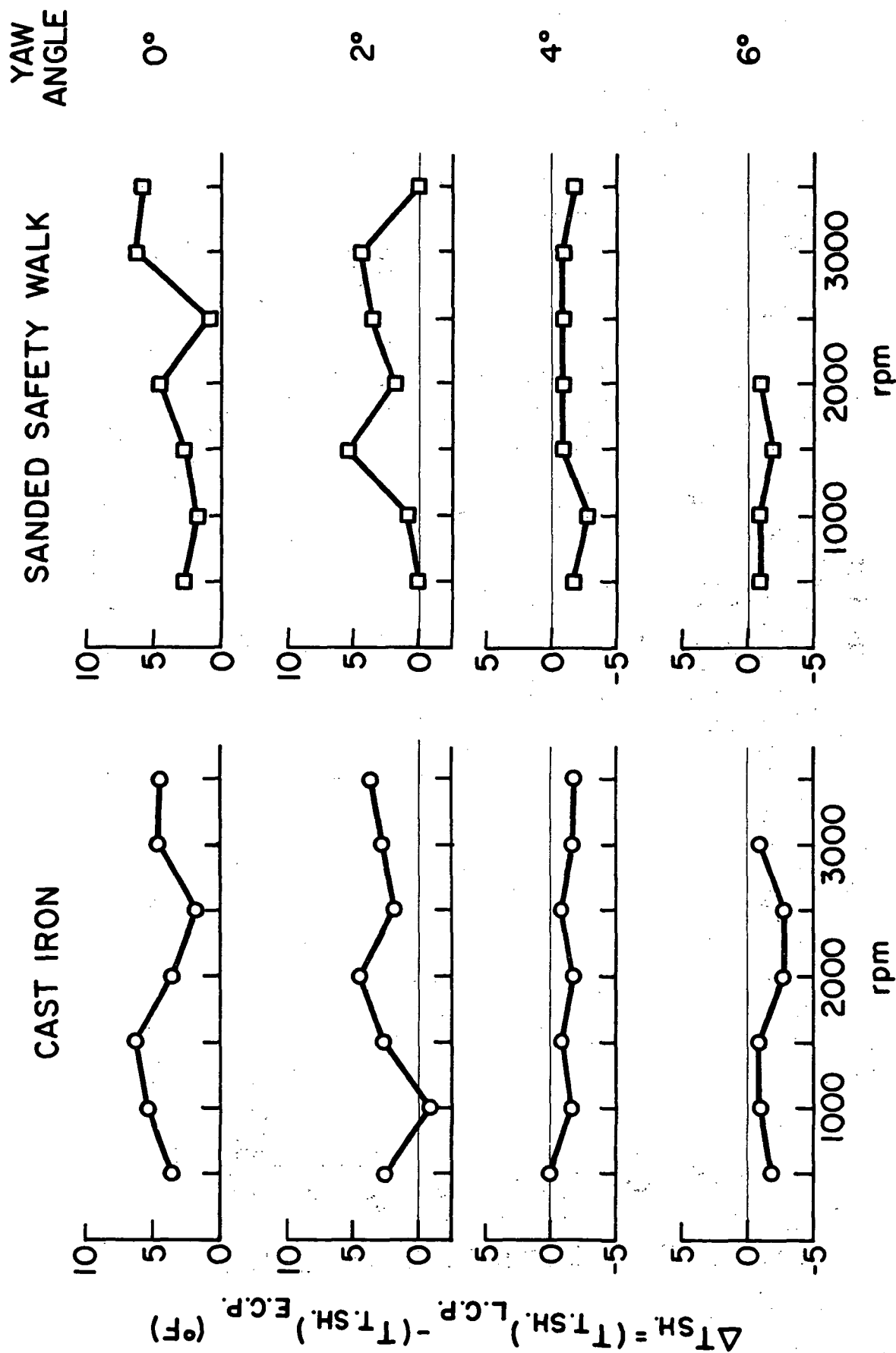


Figure 19. Temperature change of tension shoulder after going through contact patch vs. speed.

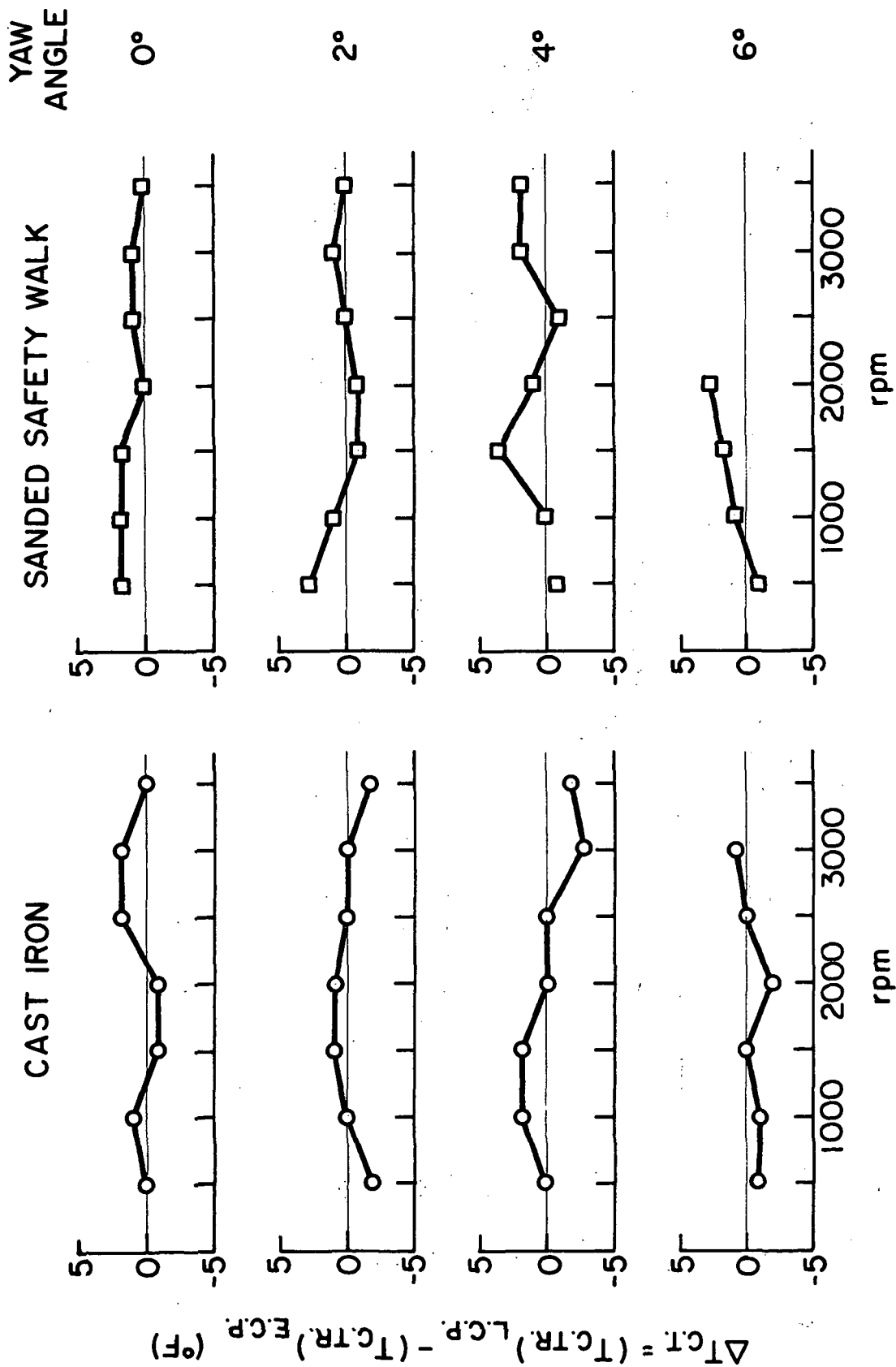


Figure 20. Temperature change of center tread after going through contact patch vs. speed.

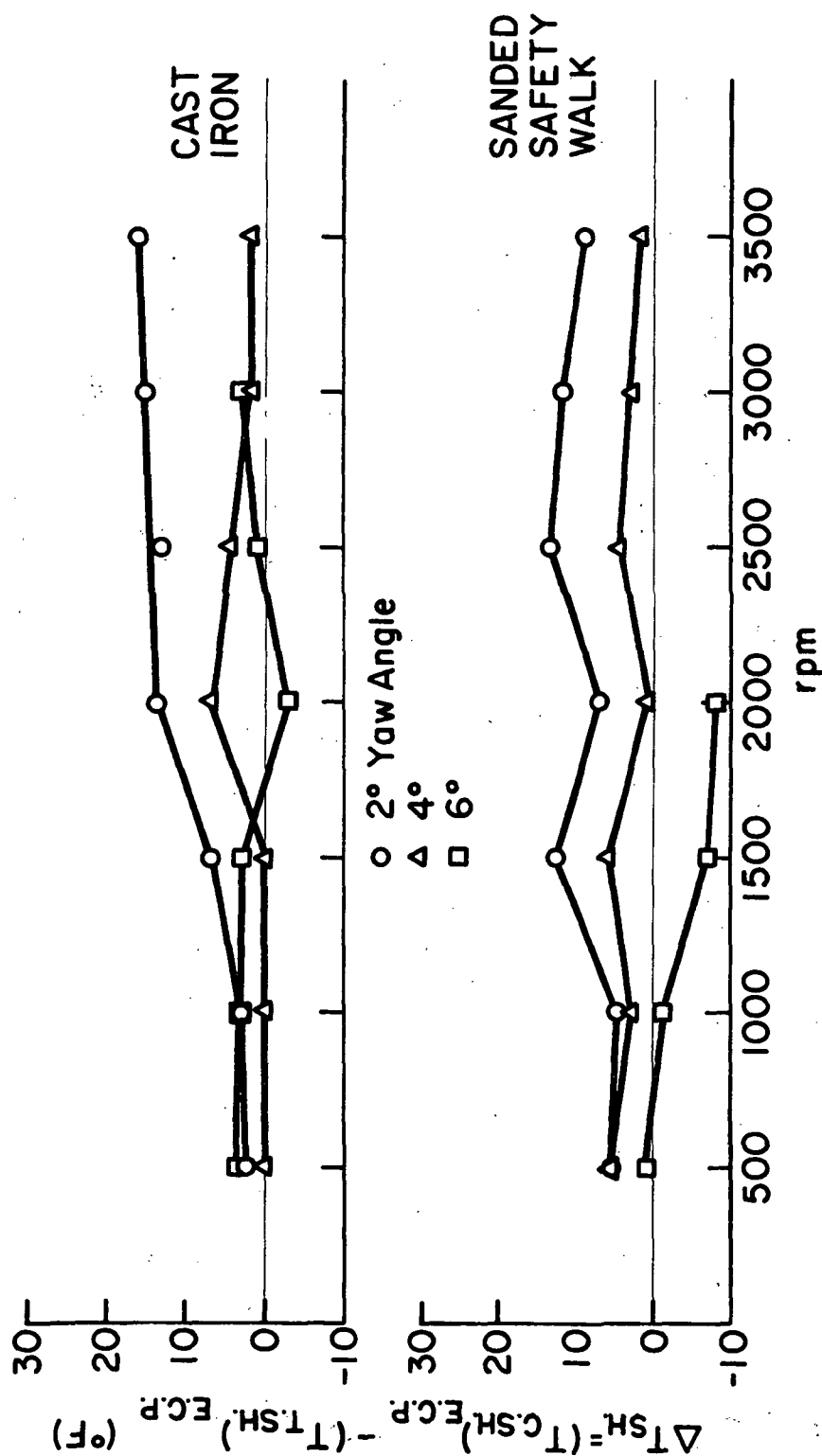


Figure 21. Temperature difference between compressed shoulder and tensioned shoulder vs. speed.

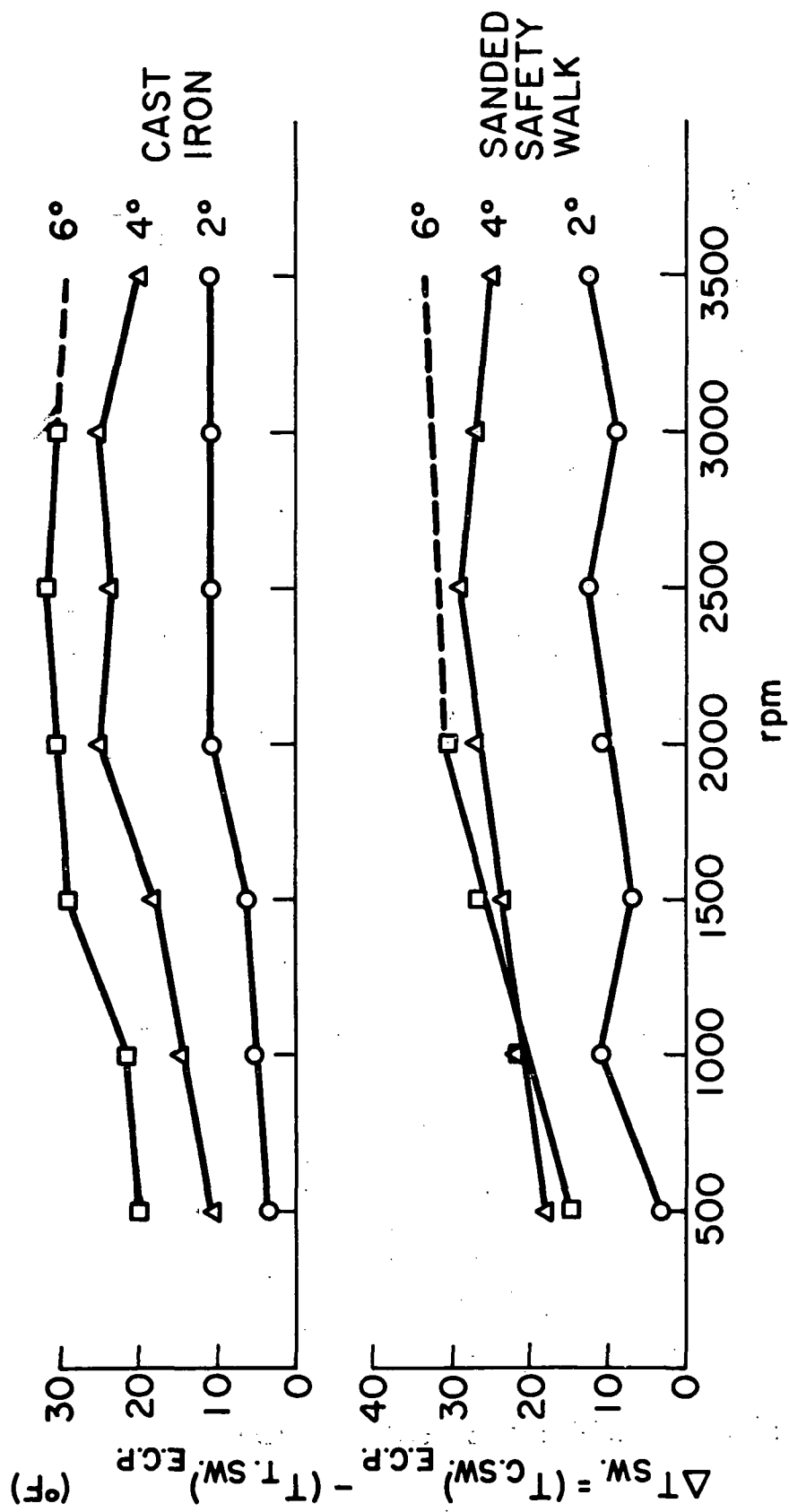


Figure 22. Temperature difference between compressed sidewall and tensioned sidewall vs. speed.

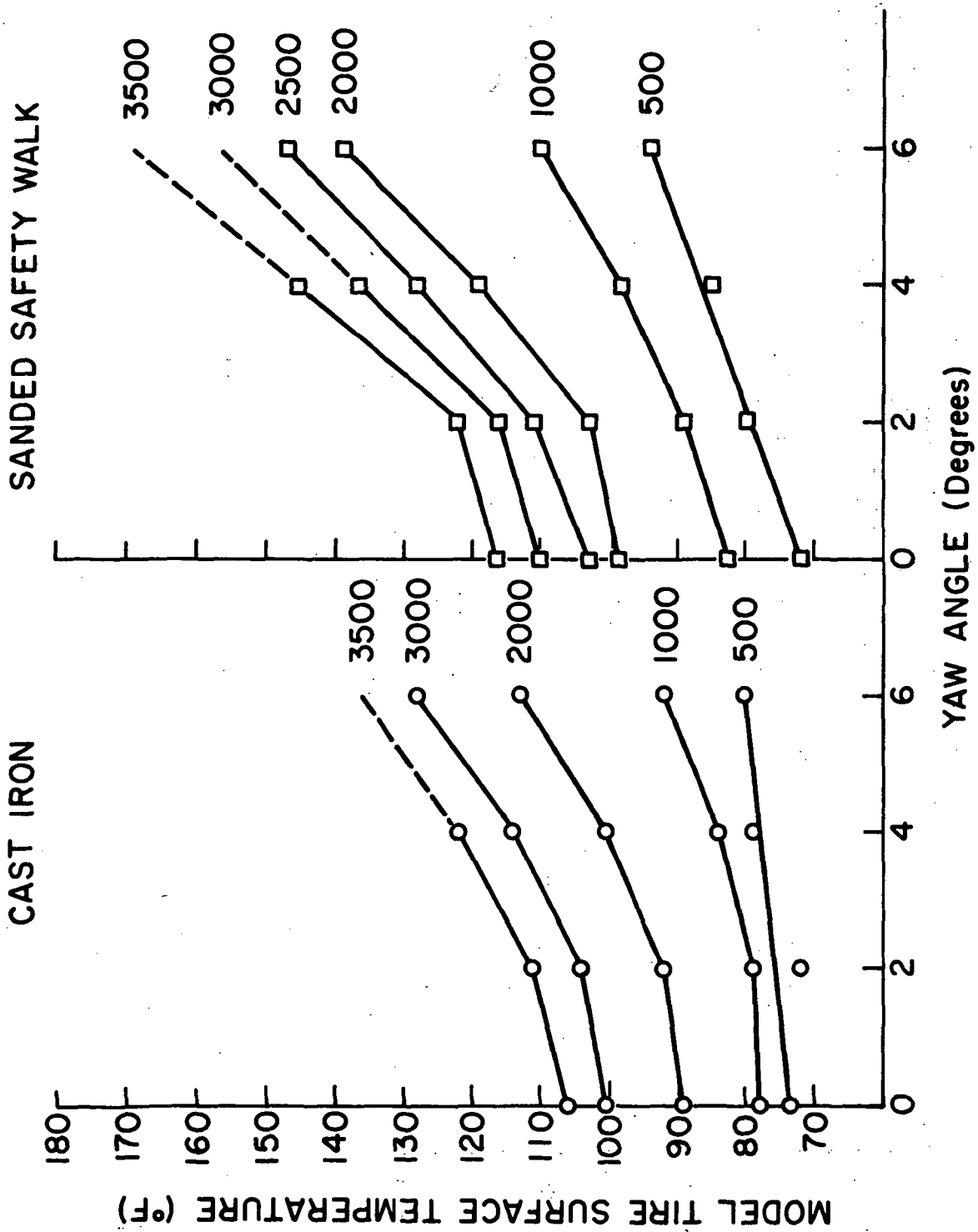


Figure 23. Center tread temperature entering contact patch.

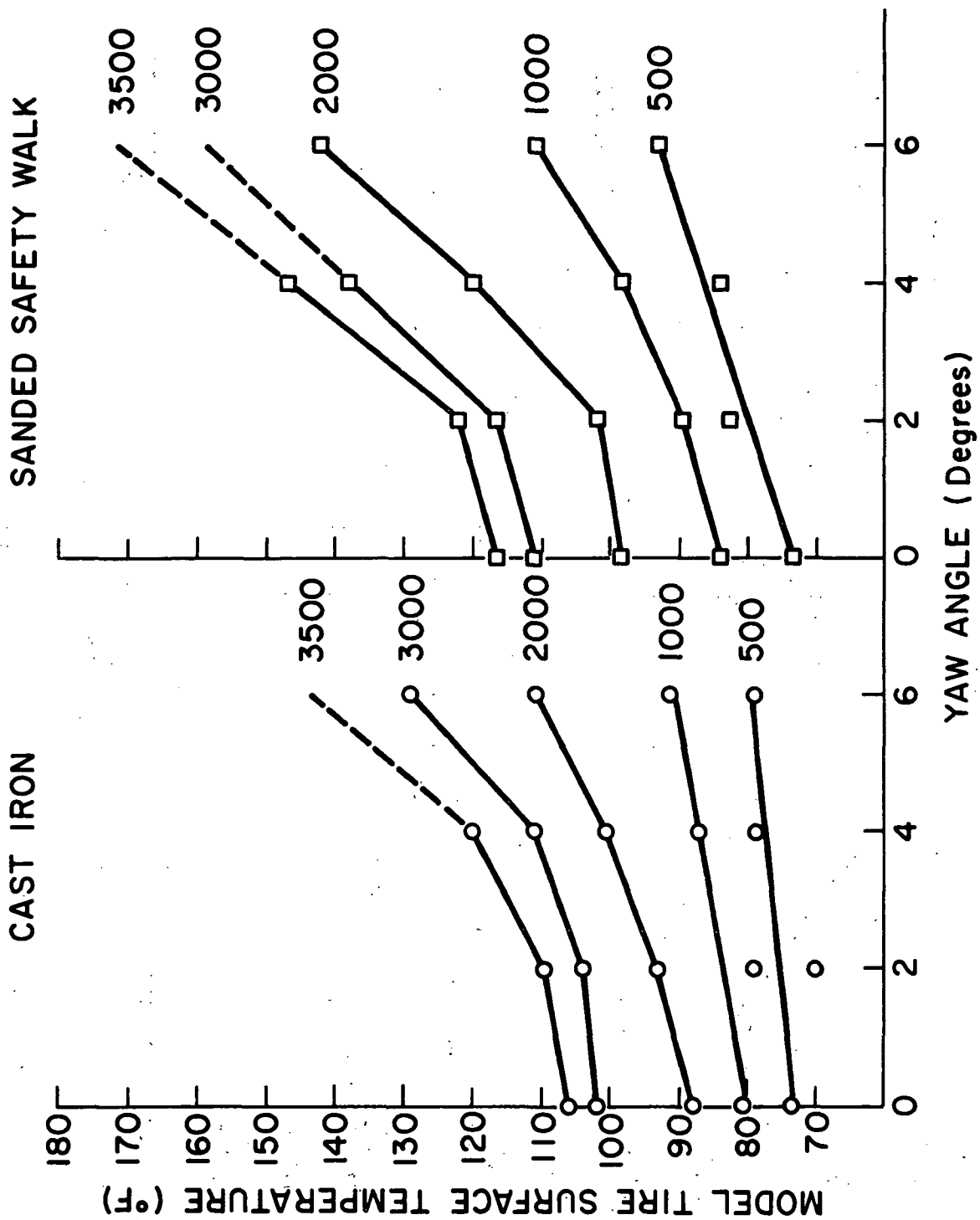


Figure 24. Center tread temperature leaving contact patch.

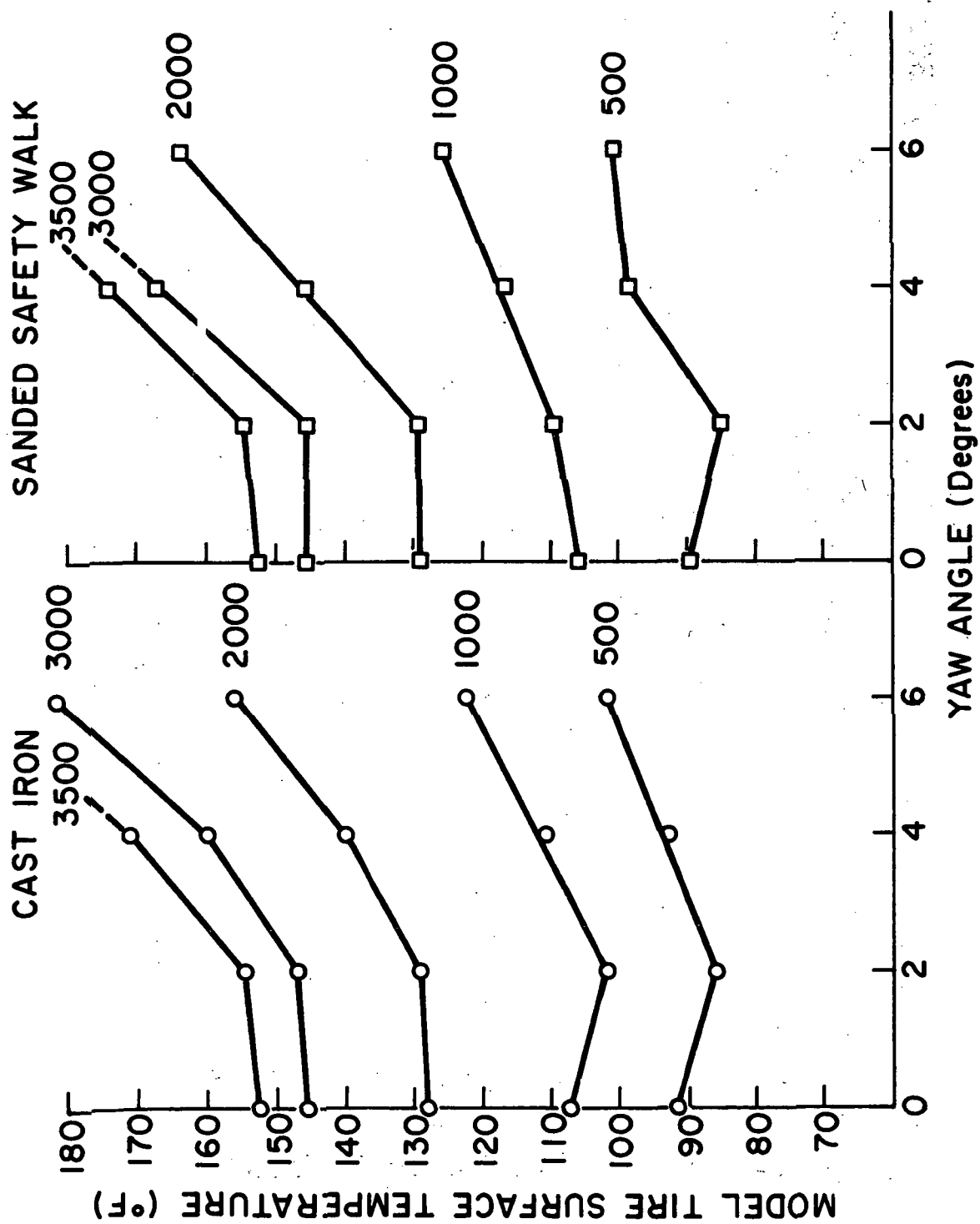


Figure 25..... Compression sidewall temperature entering contact patch.

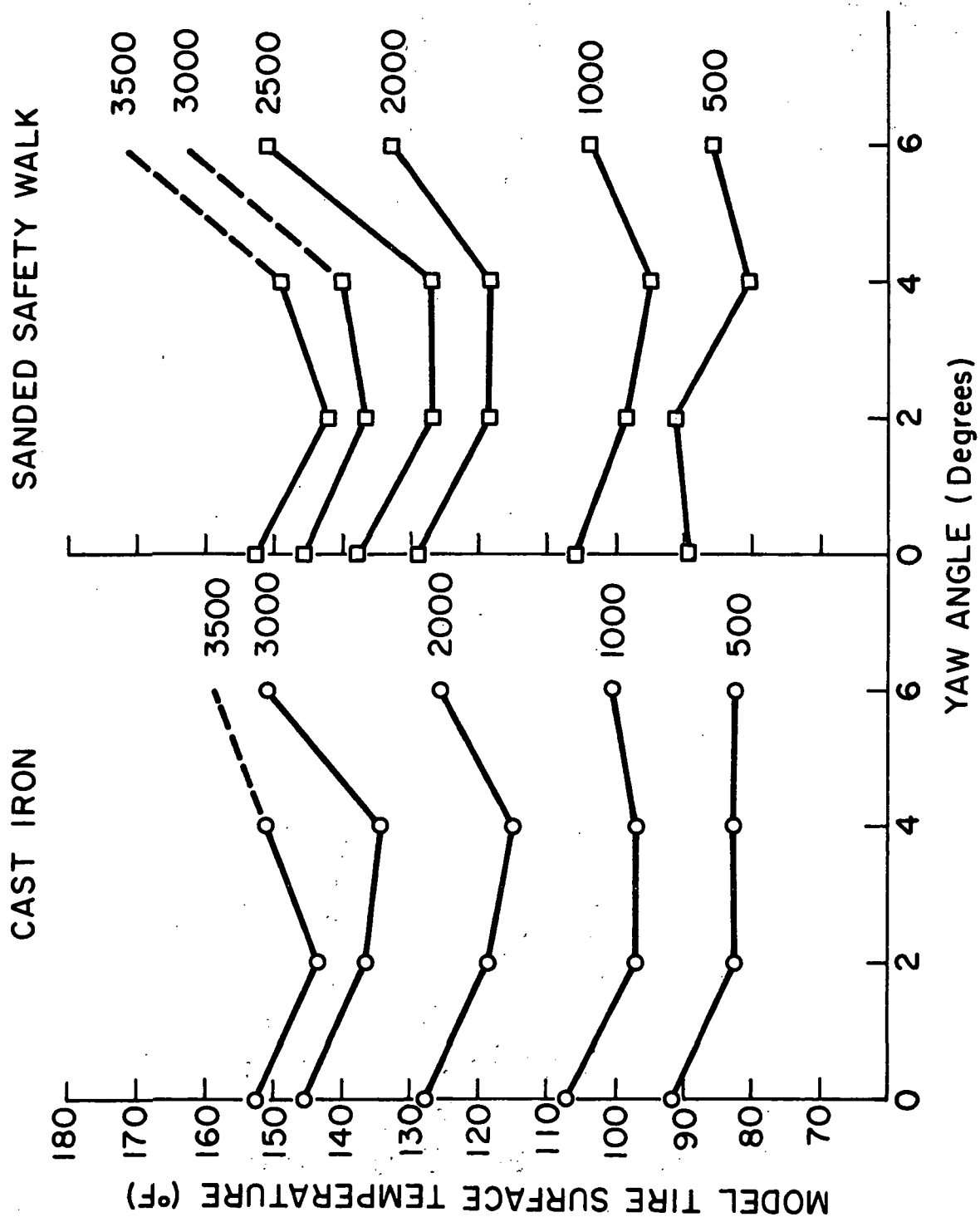


Figure 26. Tension sidewall temperature entering contact patch.

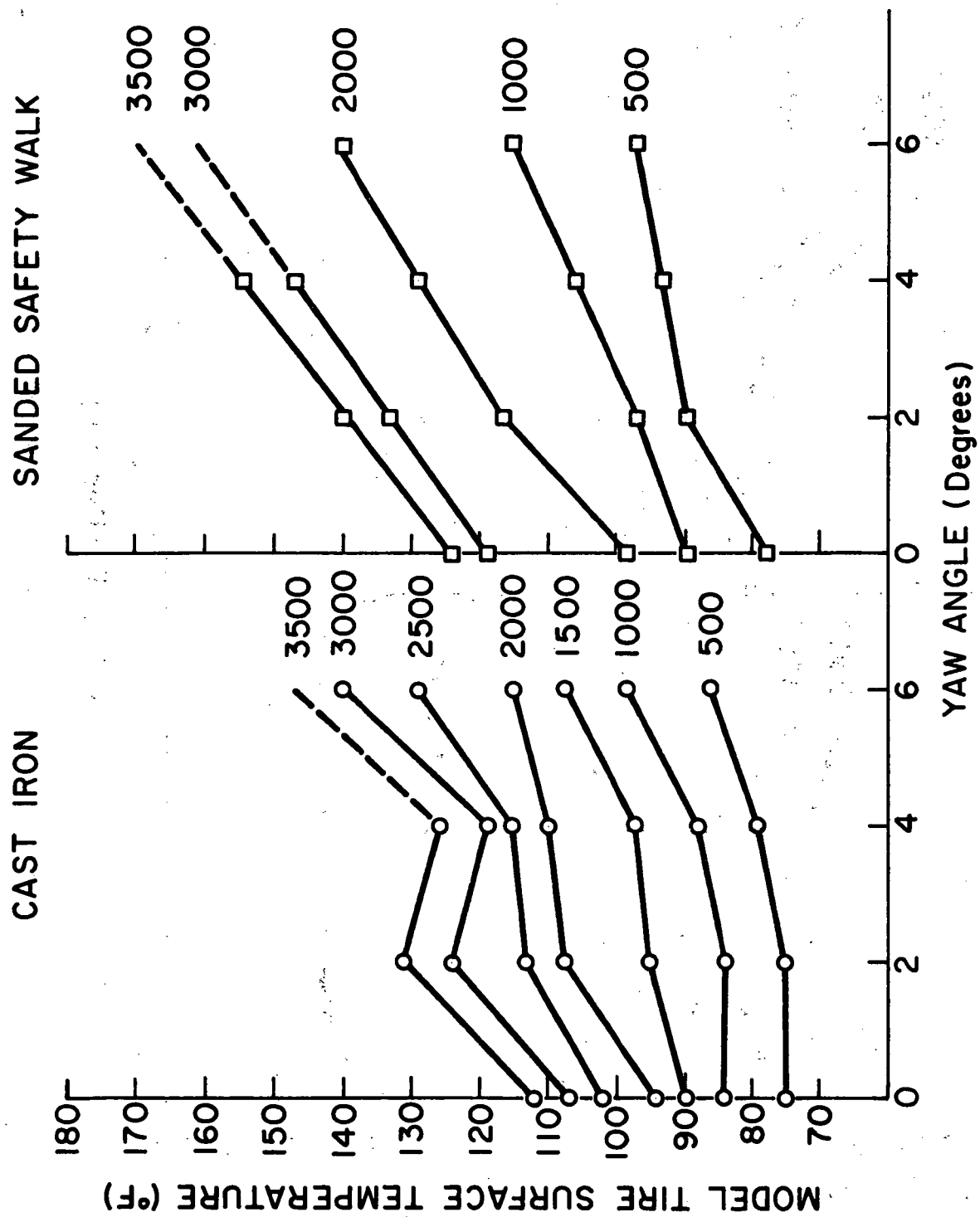


Figure 27. Compression shoulder temperature entering contact patch.

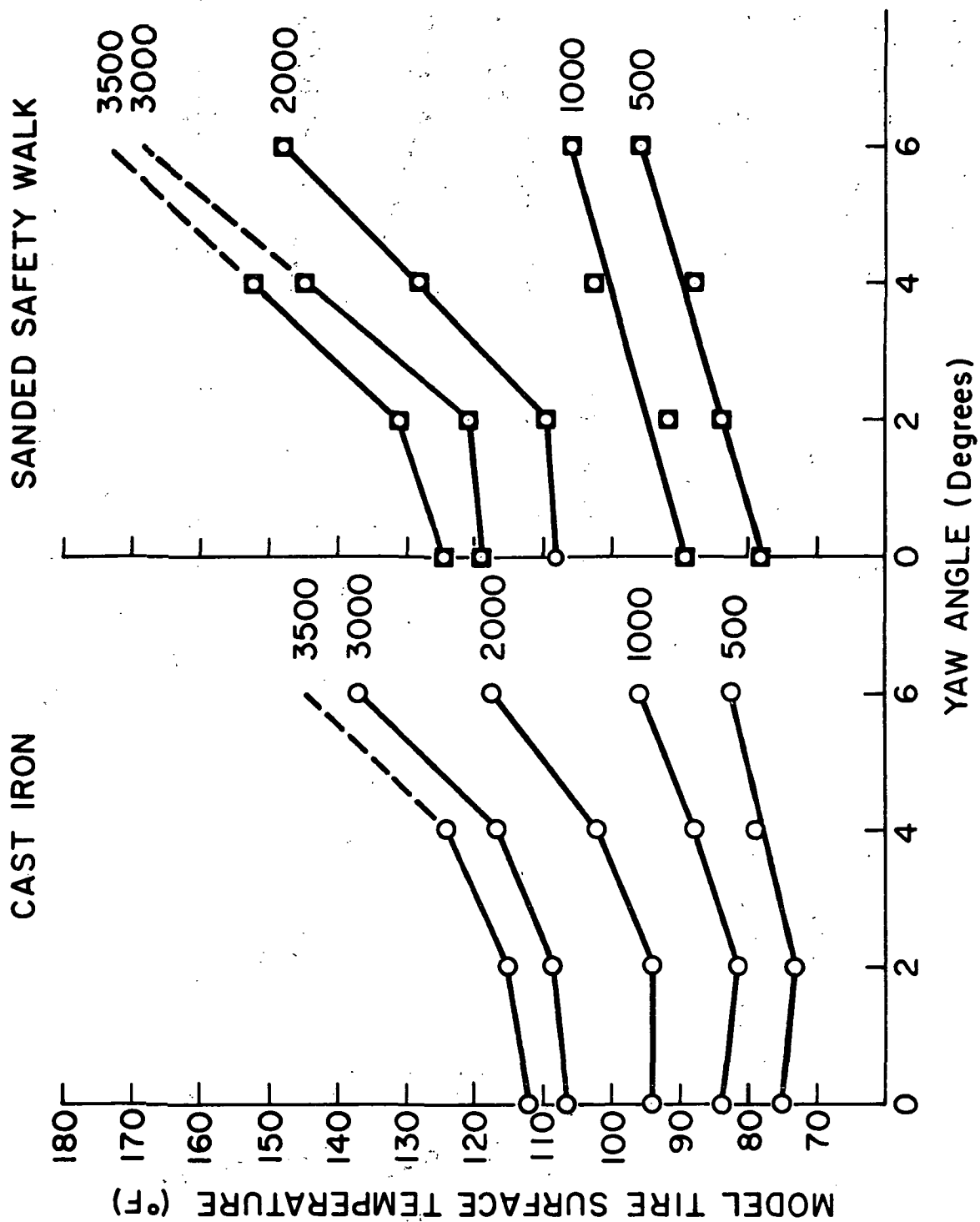


Figure 28. Tension shoulder temperature entering contact patch.

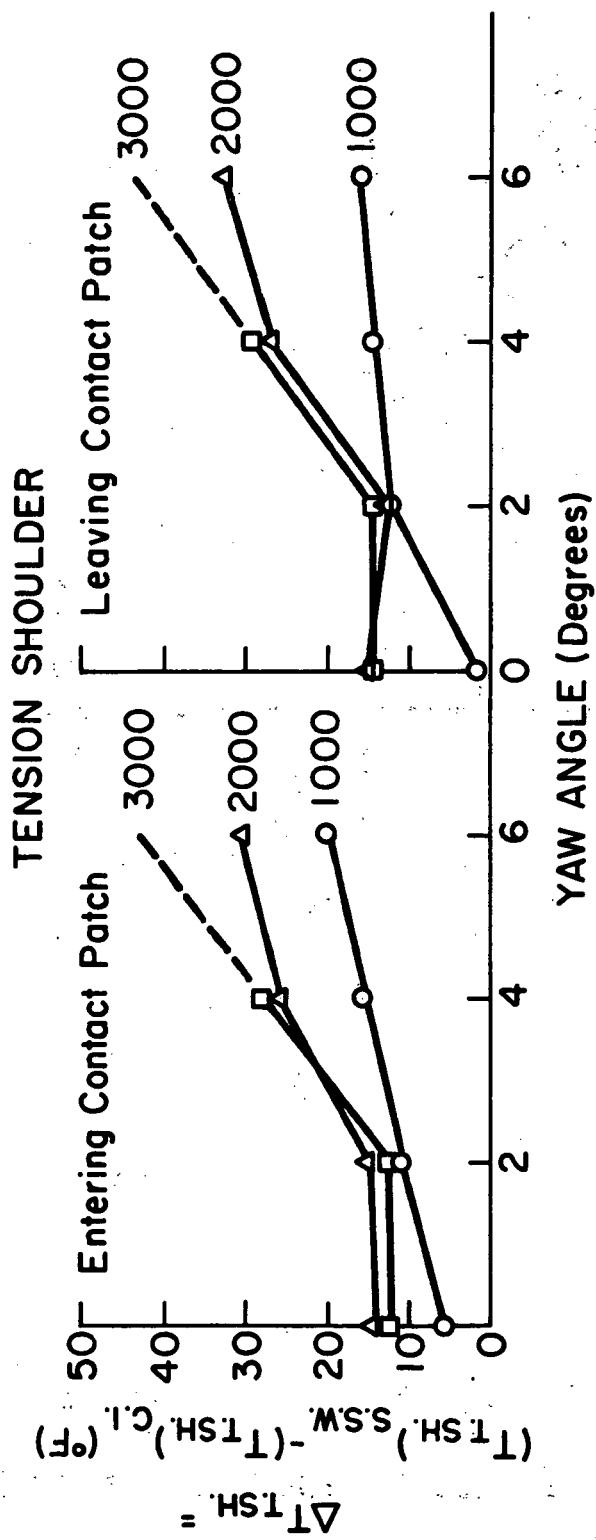
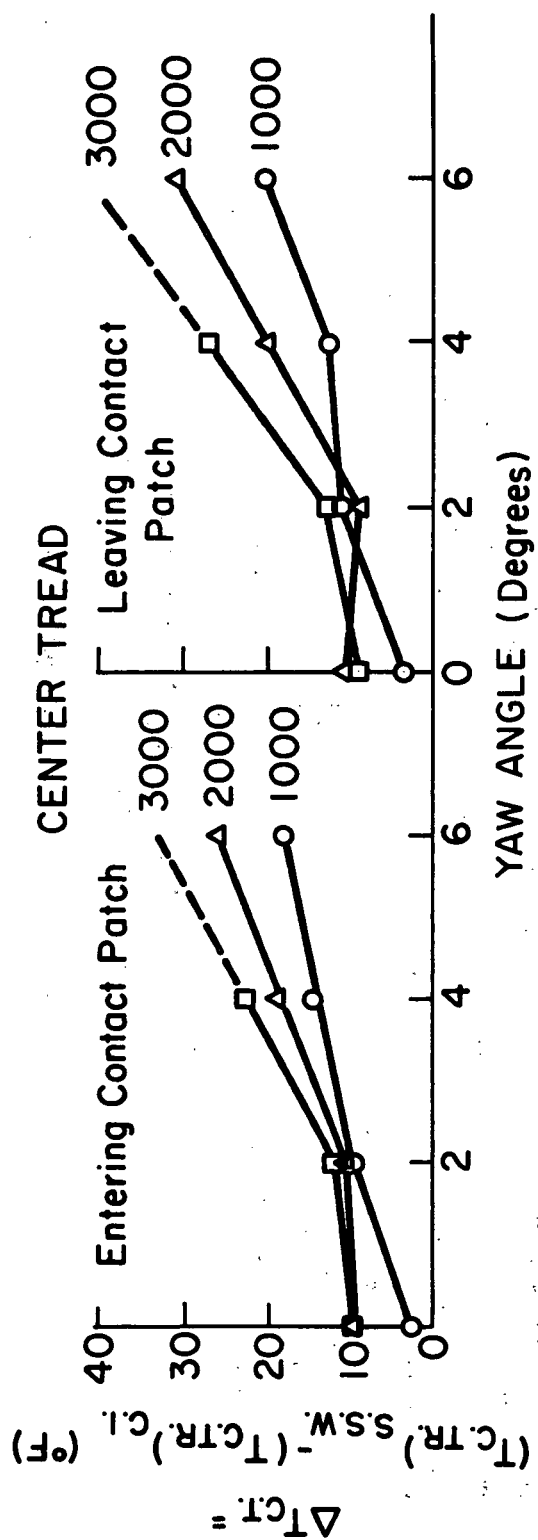


Figure 29. Temperature difference of center tread (and tension shoulder) between cast iron and sanded Safety Walk.

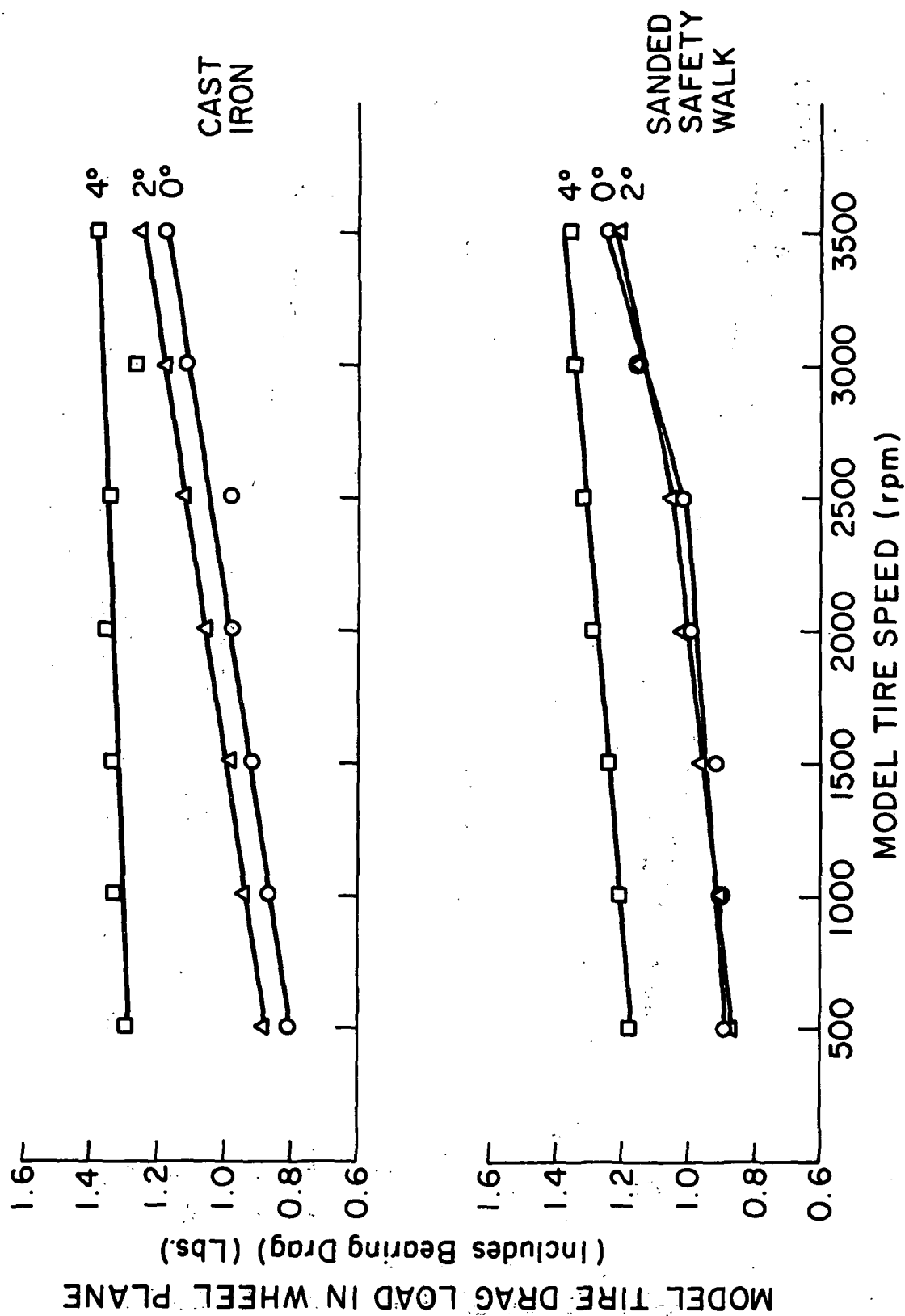


Figure 30. Drag load in wheel plane vs. speed.

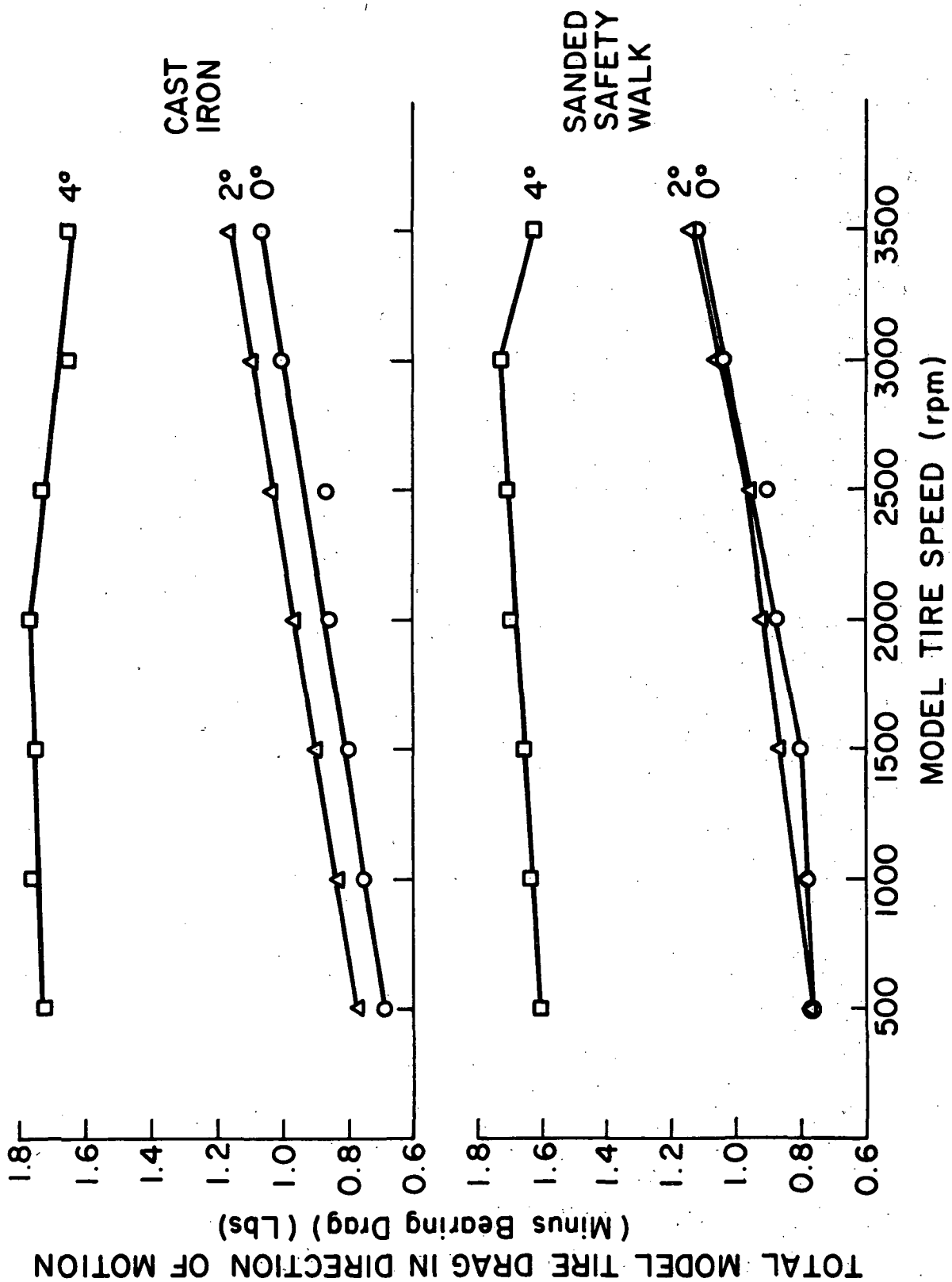


Figure 31. Drag load in direction of motion vs. speed.

VII. SUMMARY OF RESULTS

Research on this problem has been directed along three major lines of activity. These are:

- (1) An analytical study of the problem of heat conduction in the rolling tire as it contacts the roadway.
- (2) Experimental measurements on full sized tires.
- (3) Experimental measurements on small scale, model tires.

In regard to these three phases of effort, the analytical studies so far have been the least productive, at least in terms of generating new information. They have, however, been helpful in interpreting the results of some of the experiments carried out under this program. For example, a number of analytical solutions to thermal conductivity problems have been developed during the course of this one year of effort. In particular, the problem of two-body contact has been studied in some detail and a computer program written to give the temperature distribution in two bodies in contact for a short period of time, under conditions of heat release at the surface of these two bodies and under conditions of an elevated temperature of one body with respect to the other. In general this work shows that for the velocities and thermal conductivities encountered by an aircraft tire operating on a runway, the temperature profile caused by surface heating is that of an extremely thin skin on both surfaces, with the proportion of heat flowing into the concrete runway and into the tire being governed by their relative thermal conductivities and specific heats. This gives rise to the expectation that such a thermal proportioning could be radically affected by controlling the thermal properties of the runway itself,

even in the form of a very thin skin or sheet. So far, however, it has not been possible to calculate in any reasonably sound way the degree of heat released from the tire due to surface scrubbing on the runway, and so one must rely upon measured values of this quantity in order to examine the various temperature profiles exhibited.

Experiments on fully instrumented passenger car tires were carried out at the Texas Transportation Institute using The University of Michigan Highway Safety Research Institute Mobile Tire Tester. Instrumentation in these tires consisted of a large number of thermocouples embedded throughout the thickness of the tread and carcass at two regions, as well as an array of thermocouples around the meridional section of the tire. These tires were run for fairly long periods of time at a speed of 50 mph, and both the initial transient temperature rise profile and the near-equilibrium temperature distribution were measured.

From the results of the transient temperature work it has been possible to show that a large fraction of the total work done in rolling the tire under straight line, unbraked conditions is made up of hysteretic heat distributed throughout the tire carcass. However, for a cold tire far and away the largest fraction of this heat appears to be located close to the tread surface of the tire, opening up the possibility that it could be removed by some highly conductive surface mechanism.

The exact fraction of heat so generated cannot be defined quantitatively until further experiments accurately define the total drag force of the tire at the velocity and load conditions used in the thermocouple measurements.

These conclusions based on thermocouple measurements are substantiated by thin film temperature sensor measurements taken directly on the highway. A series of these measurements shows that the temperature rise associated with a freely rolling tire of typical passenger car size, at a speed of 50 mph and loaded with a vertical load of 1000 lb, was so small as to be barely measurable.

The results of these tests are not easily interpreted. It is obvious from the data recorded that the temperature of the road does not increase very much due to the passage of a free rolling tire when the tire and the road have approximately the same temperature but the mechanism of scrubbing and conduction during the time of contact remains unknown. A method for determining the magnitude and nature of the heat flux due to scrubbing, which must necessarily incorporate some scheme for separating the flux due to scrubbing from the flux due to convection, is beyond the scope of this report.

Slow speed scratch measurements were made using the same tire as used in the thermocouple measurements. These were carried out on the flat plank tire testing machine at The University of Michigan Highway Safety Research Institute, also under the same vertical load as was used on the highway tests. These measurements showed that the drag force associated with surface scrubbing of the tire was at least 5% to 10% of the total drag force of the tire. This implies that at least 5% to 10% of the energy used to move the tire forward is released in the form of surface heat scrubbing. This confirms the two previous experimental conclusions, but still leaves the possibility open that the hysteretic portion of the tire loss, which appears to be the largest portion by far, has its origin very close to the surface.

Recent computational studies on the stress states near the surface of rolling tires, such as that of Yandell [1], reinforces the idea that the distribution of hysteretic and frictional losses may be radically different in a free rolling tire and a tire rolling unbraked and yawed. Therefore, the conclusions reached so far in this work must be considered only for the case of the free rolling tire.

VIII. APPENDIX 1. THEORETICAL ANALYSIS OF SENSOR

In this appendix a simple model of the sensor is developed for the purpose of predicting the sensor response to a uniform heat flux input applied to the sensor surface as a step function. This should aid in understanding various sensor outputs. The construction and installation of the sensor are illustrated in Figure 32 and detailed in Figure 33. The simplified model is illustrated in Figure 34 where it should be noted that the epoxy layer has been incorporated into the road and the nickel film has been eliminated. The former simplification was made because the epoxy layer is very thin and because epoxy and asphalt have thermal characteristics which are the same to within the level of precision to which they are known, and to which the model is sensitive. The latter simplification was made because the conductivity of the nickel is so much greater than the conductivity of the polyimide that the thin film of nickel presents no significant resistance to the flow of heat relative to that presented by the other materials. The problem is further simplified by assuming that the system is unidimensional. This assumption is based on the fact that the width of the sensor (.125 in) is much greater than the thickness (.0015 in) and also much greater than the depth to which any significant heat penetrates during the length of time observed with the experimental equipment.

The following notation is used in the formulation and solution of the problem.

α = Thermal diffusivity, ft^2/hr

k = Thermal conductivity, $\text{BTU}/(\text{sec ft}^\circ\text{F})$

q = Heat flux, $\text{BTU}/(\text{ft}^2 \text{ sec})$

θ = Temperature, $^\circ\text{F}$

t = Time, hr

x = Distance from polyimide-road interface, ft , positive downward

L = Thickness of sensor from polyimide-air interface to polyimide-road interface, ft ; $L = e_1 + e_3$, Figure 34

1, 2 = Polyimide, asphalt

$$K = \frac{1 + \frac{k_2}{k_1} \left(\frac{\alpha_1}{\alpha_2} \right)^{1/2}}{1 - \frac{k_2}{k_1} \left(\frac{\alpha_1}{\alpha_2} \right)^{1/2}}$$

Equations and Solutions

The equations of conduction are

$$\begin{cases} \frac{\partial \theta_1}{\partial t} = \alpha_1 \frac{\partial^2 \theta_1}{\partial x^2} & -L \leq x \leq 0 \\ \frac{\partial \theta_2}{\partial t} = \alpha_2 \frac{\partial^2 \theta_2}{\partial x^2} & x \geq 0 \end{cases}$$

the boundary conditions are

$$\left\{ \begin{array}{l} -k_1 \frac{\partial \theta_1}{\partial x} \Big|_{x=-L} = \begin{array}{ll} 0, & t < 0 \\ q, & t > 0 \end{array} \quad \text{(A step function with } q \text{ constant)} \\ -k_1 \frac{\partial \theta_1}{\partial x} \Big|_{x=0} = -k_2 \frac{\partial \theta_2}{\partial x} \Big|_{x=0} \\ \theta_1(0,t) = \theta_2(0,t) \\ \theta_1(x,0) = \theta_2(x,0) = 0 \\ \theta_2(+\infty,t) = 0 \end{array} \right.$$

Solving by Laplace transforms gives us

$$\begin{aligned} x_1(x,s) &= A e^{\sqrt{\frac{s}{\alpha_1}} x} + B e^{-\sqrt{\frac{s}{\alpha_1}} x} \\ x_2(x,s) &= C e^{\sqrt{\frac{s}{\alpha_2}} x} + D e^{-\sqrt{\frac{s}{\alpha_2}} x} \end{aligned}$$

The constants A, B, C, D are determined from the boundary conditions.

The result is presented as the temperature in the polyimide as a function of position and time. Solving for $x = e_3 = .001$ in. yields the temperature at the location of the nickel film, which in this model is taken to be the temperature of the nickel film.

$$\begin{aligned}
\theta_1(x,t) = q \frac{\sqrt{\alpha_1}}{k_1} & \left\{ 2 \frac{\sqrt{t}}{\sqrt{\pi}} e^{-\frac{x^2}{4\alpha_1 t}} \cdot \sum_{n=0}^{\infty} \frac{1}{k^n} e^{-\frac{(2n+1)^2 L^2}{4\alpha_1 t}} \right. \\
& \left[\frac{1}{K} e^{-\frac{(2n+1)Lx}{2\alpha_1 t}} + e^{-\frac{(2n+1)Lx}{2\alpha_1 t}} \right] \\
& + \sum_{n=0}^{\infty} \frac{1}{k^n} \left[\frac{1}{K} \frac{x-(2n+1)L}{\sqrt{\alpha_1}} \operatorname{erfc} \left(\frac{(2n+1)L-x}{2\sqrt{\alpha_1 t}} \right) \right. \\
& \left. \left. - \frac{x+(2n+1)L}{\sqrt{\alpha_1}} \operatorname{erfc} \left(\frac{(2n+1)L+x}{2\sqrt{\alpha_1 t}} \right) \right] \right\}
\end{aligned}$$

The temperature at the surface, i.e. the temperature at the polyimide-air interface, is found by setting $x = -L$ in the above expression.

$$\theta_1(t) = 2 q \frac{\sqrt{\alpha_1}}{k_1} \frac{\sqrt{t}}{\sqrt{\pi}}$$

This is presented for reference only and has not been evaluated or plotted.

The expression for θ_1 is most easily evaluated using a computer and the results are most easily interpreted if presented in a graphical form. The computer program is straightforward and is not presented here. The evaluation has been carried out for $x = e_3 = .001$ in.

The results are shown in Figure 35 along with the results of three related problems in which the road surface is taken to be micarta, copper, and aluminum. An examination of the first 5 msec indicates that for these short times the road material has little effect on the sensor and an examination of the first 20 msec indicates that the sensor is only slightly sensitive to the distinction between micarta and concrete and asphalt. The response to a unit heat flux pulse of 6.25 msec duration has already been presented (Figure 14) and the first 6.25 msec of that figure can be taken as an expansion of the initial part of Figure 35 and examined for details if required.

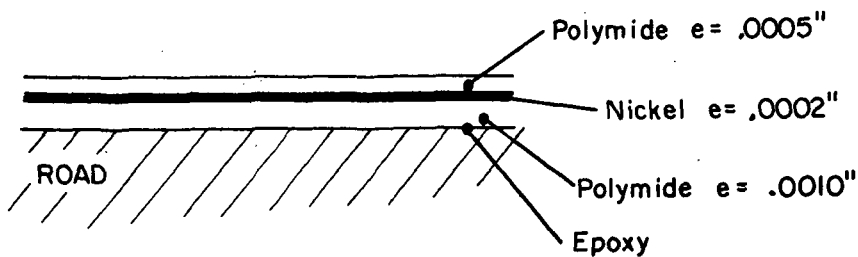


Figure 32. Detail of sensor installation.

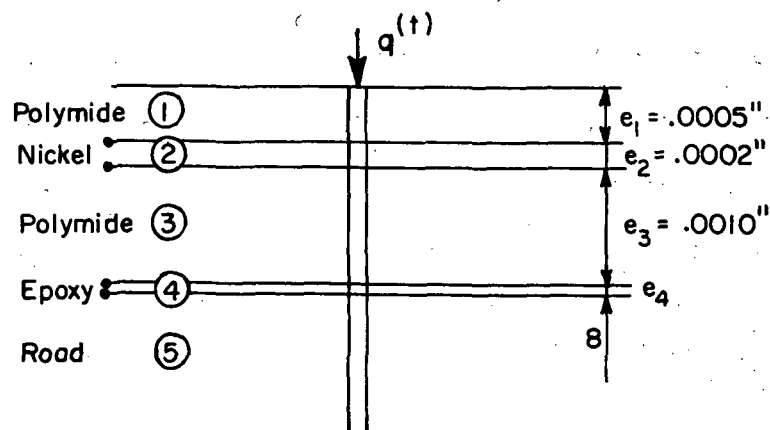


Figure 33. Schematic of sensor installation.

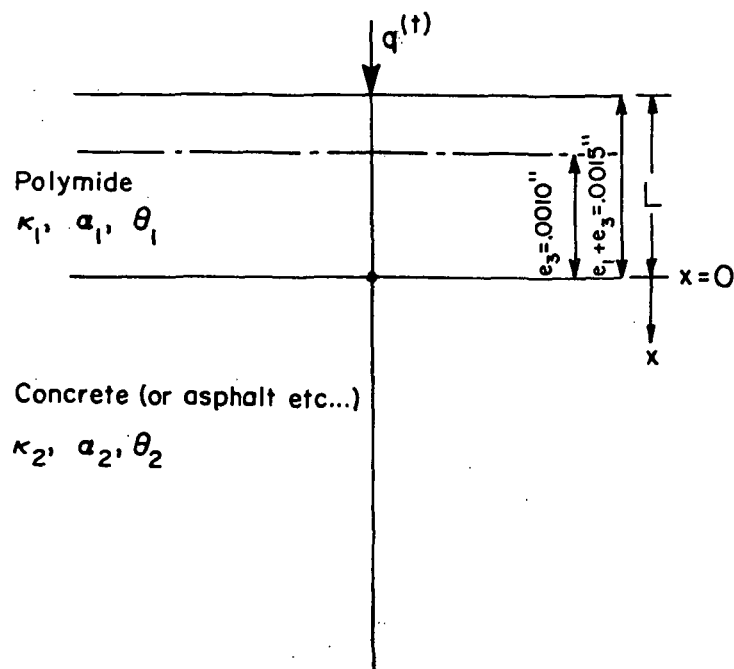


Figure 34. Analog of sensor installation for theoretical analysis.

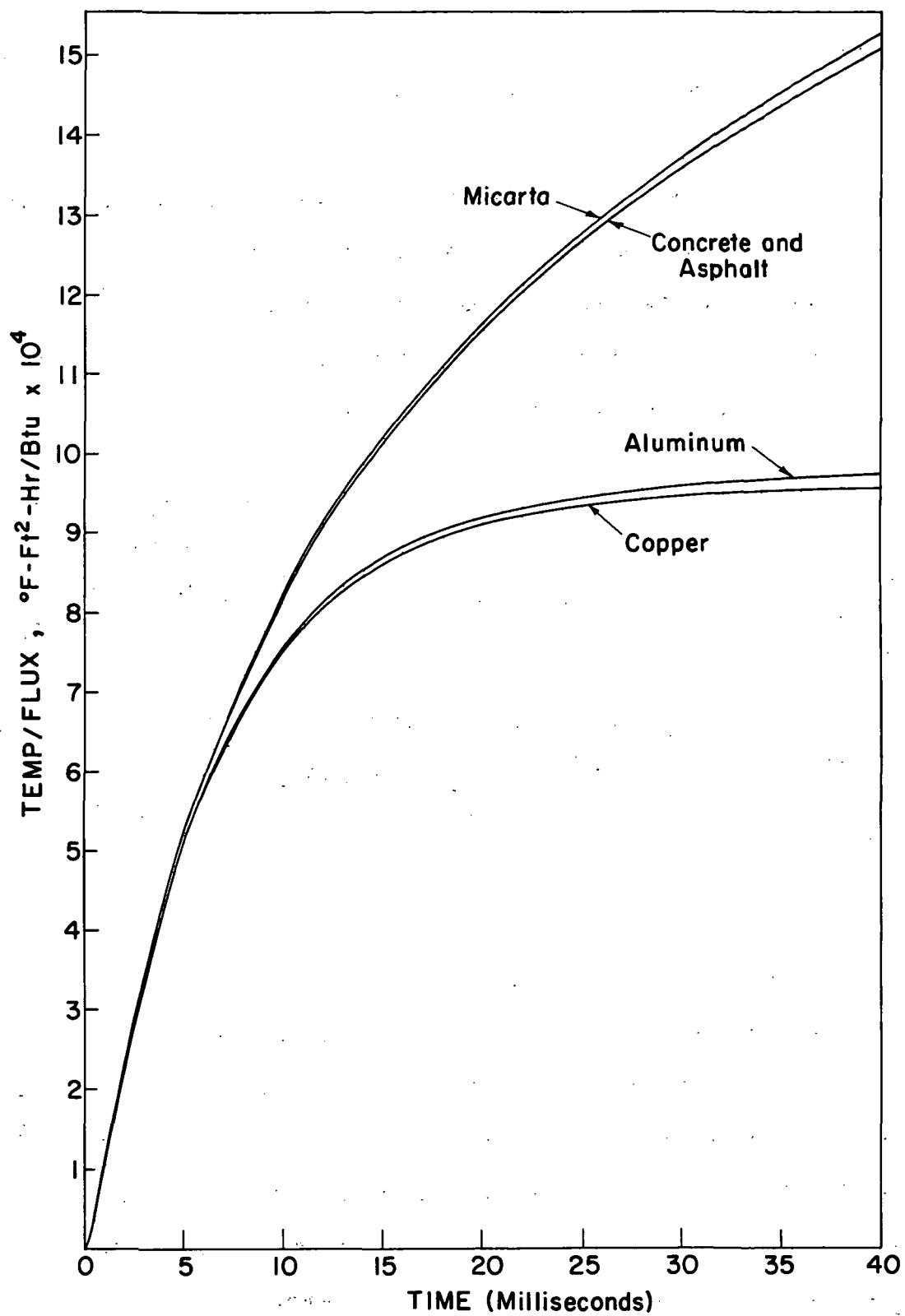
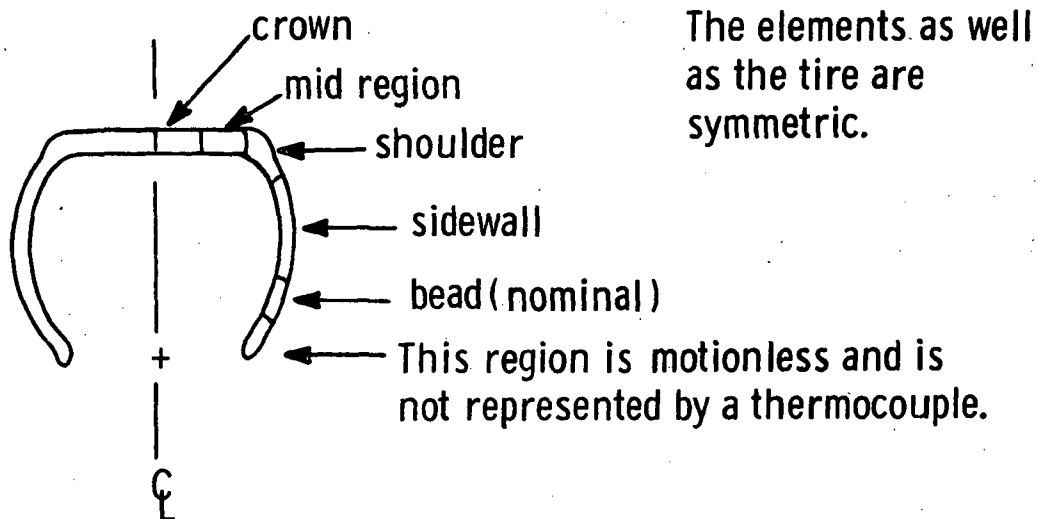


Figure 35. Temperature/flux in nickel as a function of time.

IX. APPENDIX 2. ALTERNATE METHOD OF CALCULATING HEAT GENERATION

The second scheme for determining the total rate of heat generation involves partitioning the tire cross section into elements centered about their representative thermocouples. The elements are delineated by dashed lines in Figure 1. The sketch below illustrates this partitioning and the names assigned to the elements.



The areas of the elements and the approximate distances of the centroids from the axle center can be used to calculate the representative volumes. The percentage of the total volume represented by each element becomes a weighting factor in calculating a weighted sum of the rates of temperature increase. The tire is assumed to be homogeneous so that volume fractions are equivalent to mass fractions and the specific heat capacity is taken to be that of the rubber.

The figures given are for a G78-15. All thermocouples are 1/4 in. deep. The tire weighs 30 lb. The data is for a free rolling, 50 mph experiment.

Location	% Total Volume (Left + Right Sides)	Thermocouples Averaged	$\frac{\Delta T}{\Delta t}$ avg °F/sec
Actual Bead	5.1	none	0
Bead	8.7	1,9	.1063
Sidewall	22.3	2,8	.2125
Shoulder	26.9	3,7	.2032
Mid region	22.0	4,6	.1250
Crown	15.0	5	.1188

The weighted average is $(5.1 \times 0 + 8.7 \times .1063 + \dots) \div 100$ or .1566

°F/sec. Then $Q = .1566 \times 30 \times (.48 \times 778) = 1750$ ft lb/sec. The average of all the thermocouples 1-9 = .1570

$$Q = 1759 \text{ ft lb/sec.}$$

The agreement is quite good, compared with the nonweighted method of Section III of this report.

X. REFERENCES

1. Yandell, W. O., "The Use of a Mechano-Lattice Analogy for Determining the Abrading Stresses in Sliding Rubber," Rubber Chemistry and Technology, 44, no. 3, June 1971, p. 758.
2. Viehman, W., "Surface Heating by Friction and Abrasion by Thermal Decomposition," Rubber Chemistry and Technology, 31, no. 4, 1958, p. 925.
3. Clark, S. K., R. N. Dodge, J. I. Lackey, and G. H. Nybakken, The Structural Modeling of Aircraft Tires, AIAA Paper No. 71-346, AIAA/ASME 12th Structures, Structural Dynamics, and Materials Conference, Anaheim, California, April 19-21, 1971.
4. Schallamach, A., "A Note on the Frictional Temperature Rise of Tyres," Journal of the IRI, 1, no. 1, January/February, 1967.
5. Seki, K., S. Sasaki, and H. Tsunoda, "Tyre Rolling Resistance," Automobile Engineer, pp. 88-91, March, 1969.